Original Contribution

Kurume Medical Journal, 54, 1-8, 2007

Effect of a Physical Activity Improvement Program Using the Transtheoretical Model at a Small-Scale Company

ATSUKO ISHII, MAKOTO NAKIRI, KAORI NAGATOMI, YOSHIYASU TSUJI, MICHIKO HOSHIKO, YOSHIE YAMAGUCHI, JUNKO MURAMOTO AND TATSUYA ISHITAKE

Department of Environmental Medicine, Kurume University School of Medicine, Kurume 830-0011, Japan

Received 30 October 2006, accepted 22 March 2007

Edited by KOUJI TOYOMASU

Summary: The present study aimed to investigate the potential use of the transtheoretical model (TTM) by clarifying the program's effects on workers at a small-scale company. Subjects were 22 male workers at a communication system company. They were divided into two physical activity improvement program groups, the TTM-based assistance group (TTM group, n=12) and the control group (n=10). During the study period each subject was asked to wear a calorie counter and to record daily exercise. Changes in number of steps per day and body weight were measured before, immediately after, and 1 month after the intervention ended. Stage of exercise behavior, health protective behavior, and self-efficacy were also examined by means of self-administered questionnaires. In the control group, the number of steps per day tended to increase immediately after the intervention and then decreased at 1 month after the program ended. In both groups, physical activity peaked during commuting and lunch hours. This peak persisted for 1 month after the intervention in the TTM group, but not in the control group. Moreover, the stage of exercise behavior tended to progress in the TTM group, whereas regression in the stage of exercise behavior was observed in the control group. In the control group, although the exercise self-efficacy score after intervention was higher than that before intervention, the health protective behavior score decreased at 1 month after the program ended. This study suggested that physical activity improvement programs based on TTM may be useful for workers at small-scale companies. However, further study of larger numbers of workers will be needed to confirm the validity and usefulness of these results.

Key words transtheoretical model (TTM), small-scale company, physical activity improvement program

INTRODUCTION

In Japan, companies with 50 or more employees are legally required to have an occupational safety and health management system composed of a general safety manager, health officer and industrial physician by the Industrial Safety and Health Act [1]. However, small-scale companies with less than 50 employees are exempted from this requirement. In addition, many small-scale companies face underlying issues such as weak management foundations, an older workforce, and a lack of individuals with specialized knowledge in occupational safety and health. Both employers and employees at small companies tend to be less aware of industrial health activities, or in other words, industrial health activities are not actively being implemented [2]. Under such circumstances, regional occupational health centers have been established by the government to provide occupational health services to small-scale companies. These services include follow-

Address for correspondence: Atsuko Ishii, Department of Environmental Medicine, Kurume University School of Medicine, 67 Asahi-machi, Kurume 830-0011, Japan.

Abbreviations: A, action; BMI, body mass index; C, contemplation; M, maintenance; PC, precontemplation; PR, preparation; TTM, transtheoretical model.

TABLE 1.
Stage of exercise behavior

Precontemplation (PC)	I have not exercised and do not intend to exercise.
Contemplation (C)	I have not exercised but intend to exercise within 6 months.
Preparation (PR)	I exercise but not regularly.
Action (A)	I have been exercising less than 6 months.
Maintenance (M)	I have been exercising more than 6 months.

up health consulting after health examinations and providing occupational health information [3-5].

"Healthy Japan 21" is a national program aimed at promoting the health of Japanese citizens in the 21st century. This program stresses the importance of physical activity for the prevention of lifestyle diseases and the promotion of health, and concrete numerical targets have been established [6]. However, less than 30% of males in their 20's through 50's exercise regularly, according to the national health and nutrition survey [7]. At present, various studies are being conducted to ascertain the effects of physical activity on health, but systematic assistance programs to improve physical activity have not been established.

Table 1 shows the stages of exercise behavior. This applies the transtheoretical model (TTM) proposed by Prochaska et al. [9] to exercise, and is one behavioral science model that has been widely used in Western countries [8-12]. Stages were classified according to baseline exercise conditions and the level of preparation for behavioral modifications. A different approach depending on the stage of subject has been reported to be a valid intervention [13-15]. The objective of this study is to clarify the effectiveness of a TTM-based physical activity improvement program for workers in a small-scale company.

MATERIALS AND METHODS

Subjects

Thirty-eight male workers in a communication system company were enrolled. They were divided into two groups: a TTM group of 18 subjects who received individual guidance based on the TTM and a control group of 20 subjects who received general group guidance by adjusting the program starting time and the hours of instruction during work hours. We used the data of 12 workers in the TTM group and 10 workers in the control group for analysis because of incomplete data quality. No calorie counter data was missing during the study period, and all questionnaire items were answered before and after intervention and at 1 month after the end of the program in these 22 subjects. No significant difference was observed in the mean age of workers between the two groups (39.0±8.3 years in TTM group vs. 41.7±5.1 years in control group).

The physical activity improvement program was implemented and results were surveyed after obtaining informed consent by explaining the study objectives and contents. The same exercise program was administered to both groups, but the programs were administered at different time periods.

The physical activity improvement program

Figure 1 shows a flowchart of the physical activity improvement program for each group. The study period was from early May 2004 to early August 2004. During this period, each subject was asked to wear a calorie counter (OMRON health counter HJ-710IT) and to record daily exercise in a chart. As far as exercise was concerned, individual goals were set based on lunchtime walking and "*Nagara-type*" exercise. *Nagara* exercise converts daily life activities into effective exercise while commuting, working, doing housework, or shopping [16]. In addition, once every week, data were downloaded from the calorie counters and were organized into weekly and daily records and presented to the subjects. At the workplace, the overall mean number of steps per day for each group was presented in the form of figures. In addition, for the control group, TTM-based individual guidance was provided 1 month after the program ended.

The TTM group received guidance in the form of special documents containing various types of advice that were prepared individually, and individual guidance was provided to match the characteristics of each stage of exercise behavior. On the other hand, the control group received general group guidance on the benefits and methods of exercise. The following points were emphasized for each respective stage of TTM based guidance [13,17,18].

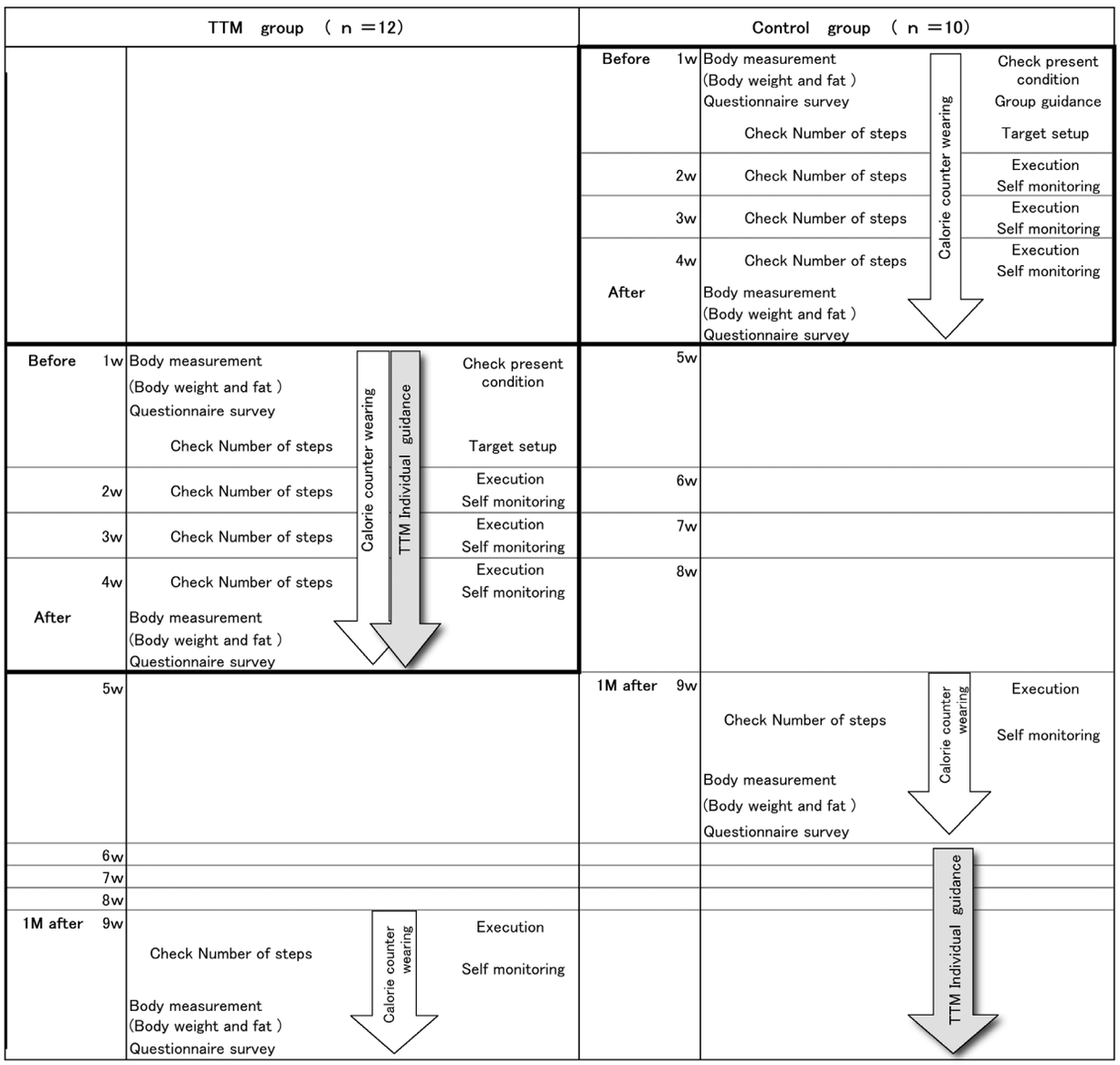


Fig. 1. Flowchart of the physical activity improvement program in the TTM and control groups.

Precontemplation and contemplation (PC, C) stages

For workers in the PC or C stage, the program was designed so that they could objectively recognize their own physical activity through measures such as self-monitoring of steps, while being part of a group with the same goals.

Preparation, action, and maintenance (PR, A, and M) stages

Workers in the PR stage were exercising but not regularly. In general, guidance can easily lead to behavior modification for people in this stage, and interventional effects are the greatest among the five stages. However, some workers in this stage might have attempted to exercise but failed in the past, and it was necessary for them to realize that they could succeed in exercising regularly. They were given opportunities to receive self-rewards when their goals were achieved. Furthermore, in order to maintain and reinforce new exercise habits, workers were given praise and encouragement when their goals were achieved.

Workers in the A or M stage were already exercising regularly, and the program was designed to allow them to continue their exercise and add exercises that were considered necessary. For workers in these stag-

es, continuing to exercise was influenced not only by receiving support, but also by exercising with other people. Therefore, the program was designed to allow workers to be with other subjects who had the same goals so that they could obtain new information, incorporate them into their own exercise routines, and act as role models for others to prevent regression.

Investigated items

The following items were investigated in both the TTM and the control groups: number of steps per day, body weight and fat, body mass index (BMI), stage of exercise behavior, health protective behavior, and general and exercise self-efficacy. For stage of exercise behavior, subjects were asked to choose one of the defined stages of exercise. Regular exercise in this study was defined as exercise for 30 min or longer per session, twice a week [7].

Health protective behavior was defined as behavior that was performed for prevention and early detection of diseases in the absence of subjective symptoms or apparent diseases. In other words, health protective behavior included eating well, sleeping and resting sufficiently, and improving their surrounding environment to prevent diseases without having subjective symptoms. The 21-items of health protective behavior prevention scale developed by Munakata was used [19].

Self-efficacy is an individual conviction that one is able to efficiently achieve a certain task [20]. General self-efficacy scales have been developed to measure the degree of general self-efficacy in daily living. In the present study, the 16-items scale developed by Sakano [21] was used. With this scale, the higher the score, the higher the general self-efficacy. However, general self-efficacy scales are not used alone, should be used with a scale developed for a specific behavior [22]. Hence, the exercise self-efficacy scale developed by Oka [23] was utilized with the above-mentioned general self-efficacy scale. When placed in a situation in which exercise was possible, subjects answered whether or not they could regularly exercise in five grades from "Do not agree at all (1)" to "Totally agree (5)".

Statistical analysis

For the TTM and the control groups, the mean number of steps per day before intervention (1 week), after intervention (4 week), and 1M after the end of intervention were compared using one-way ANOVA. Multiple comparison by the Bonferroni method was performed when effects of the program were observed from ANOVA. Moreover, changes in scores for the five items (body weight and fat, health protective behavior, general self-efficacy and exercise self-efficacy) were analyzed at the three time points in the same manner: before intervention, after intervention, and at 1M after the end of the program. All analyses were carried out using SPSS 11.5J (SPSS Japan Inc.).

RESULTS

Changes in the number of steps per day

Table 2 shows the mean number steps per day for each group. For the TTM group this number tended to increase, but differences at the three time points were not significant. On the other hand, for the control group, there were significant differences ($F_{(4,36)}$=6.44, $p<0.05$), and results of the multiple comparison tests showed that the number of steps per day after intervention tended to be higher than before intervention or at 1M after the program ended.

Figure 2 shows the diurnal changes in number of steps at the three time points. The bar graph indicates mean number of steps per hour for a week. For the TTM group, before intervention, the number of steps per day was highest during the 9th hour of the day

TABLE 2.
Change in number of steps per day in the TTM and control groups

	Before	Intervention		After	1 M after end of program	Effect of time	Multiple comparison test
	1 week	2 week	3 week	4 week			
TTM group n=12	4890.1 (2107.72)	5589.0 (1641.54)	5357.8 (1097.62)	6498.2 (1651.57)	6060.4 (1490.86)	†	n.s.
Control group n=10	4716.7 (1587.56)	5124.5 (2063.15)	6482.3 (2564.22)	7142.4 (2712.30)	5110.4 (1494.56)	*	† Before < After † 1 M after end of program < After

$p<.05$, † $p<.10$, Mean (SD)

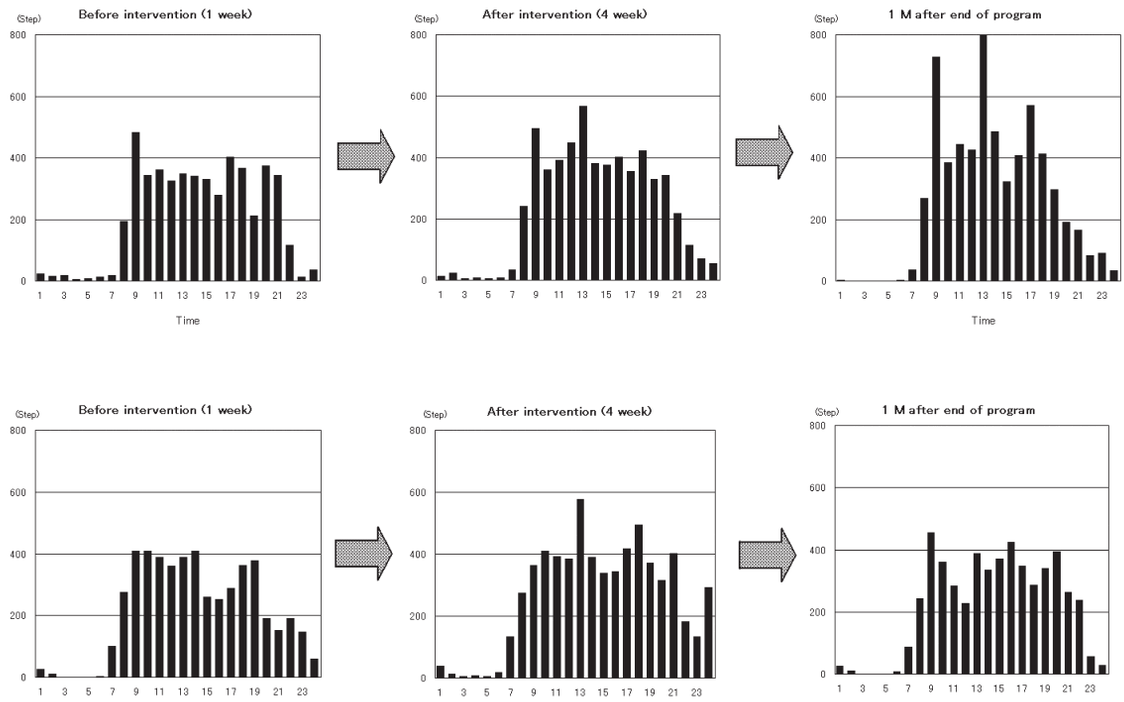


Fig. 2. Diurnal changes in mean number of steps at three time points in the TTM and control groups.

because some people were commuting on foot rather than in vehicles. While on the program, the number of steps per day was the highest during the 13th hour of the day since the workers walked during lunchtime, and it was second highest during the 9th hour of the day. At 1M after the end of the intervention, peaks continued to be observed at the 13th, 9th, and 18th hours of the day, indicating that the workers were continuing to walk during their commute and lunch hours. On the other hand, in the control group, no characteristic diurnal changes in the number of steps per day were seen before intervention, but during the program, as in the TTM group, the number of steps per day was the highest during the 13th hour of the day (lunchtime), followed by the 18th hour of the day (walking home). However, in the control group 1M after the end of the intervention, the number of steps per day was the highest during the 9th hour of the day, but no peaks were observed during the 13th or 18th hours.

Changes in stage of exercise behavior

Table 3 shows changes in stage of exercise behavior before and after intervention for each group. In the TTM group, one worker changed from PC to C and one from C to A. In the control group, one worker changed from PC to C, one from PC to PR, one from C to PR and two from PR to A. However, in this group, one worker regressed from A to PR.

Table 4 shows changes in stage of exercise behavior between the point immediately after intervention and one month after the end of the program for each group. In the TTM group, one worker changed from PC to C, one from C to PR, and two from PR to A. In the control group, three workers regressed; one from C to PC, one from PR to C, and one from A to C. Hence, at 1M after the end of the program, the TTM group showed continued progression, whereas regression tended to occur in the control group.

Changes in body weight and fat, BMI, health protective behavior, general self-efficacy, and exercise self-efficacy

Table 5 shows changes in several investigated items at three time points for the TTM and control groups. For the TTM group, no significant differences existed for any of the items.

On the other hand, in the control group significant changes were observed in health protective behavior, ($F_{(2,18)}$=5.35, $p<0.05$), and in the <mental stress> ($F_{(2,18)}$=7.74, $p<0.01$) and <vacation> ($F_{(2,18)}$=4.04, $p<0.05$) components of exercise self-efficacy. The results of multiple comparison tests showed a significant

TABLE 3.
Change in stage of exercise behavior before and after intervention in the TTM and control groups

		TTM group		After intervention			Control group		After intervention		
Before intervention	Stage of exercise behavior	PC	C	PR	A	M	PC	C	PR	A	M
	PC (Precontemplation)	2	1				1	1	1		
	C (Contemplation)		2		1			0	1		
	PR (Preparation)			2					3	2	
	A (Action)				2				1	0	
	M (Maintenance)					2					

TABLE 4.
Change in stage of exercise behavior after intervention and at 1 M after end of program in the TTM and control groups

		TTM group		1 M after end of program			Control group		1 M after end of program		
After intervention	Stage of exercise behavior	PC	C	PR	A	M	PC	C	PR	A	M
	PC (Precontemplation)	1	1				1				
	C (Contemplation)		2	1			1	0			
	PR (Preparation)			0	2			1	5		
	A (Action)				3			1		1	
	M (Maintenance)					2					

TABLE 5.
The change in several investigated items at three time points in the TTM and control groups

Item	TTM group (n=12)					Control group (n=10)				
	Before intervention	After intervention	1 M after end of program	Effect of time	Multiple comparison test	Before intervention	After intervention	1 M after end of program	Effect of time	Multiple comparison test
Weight <kg>	66.6 (10.72)	65.9 (10.28)	66.6 (10.70)	n.s.	–	68.7 (9.84)	69.0 (9.86)	68.9 (10.19)	n.s.	–
Rate of body fat <%>	20.9 (4.53)	20.9 (4.81)	20.6 (5.10)	n.s.	–	23.9 (2.63)	23.1 (3.84)	23.4 (3.22)	n.s.	–
Body mass index	23.3 (2.22)	23.1 (2.18)	23.3 (2.26)	n.s.	–	23.3 (2.27)	23.4 (2.32)	23.4 (2.44)	n.s.	–
Health protective behavior	9.9 (3.94)	12.4 (5.05)	12.3 (4.49)	n.s.	–	9.9 (3.38)	11.5 (2.99)	9.0 (4.47)	*	∗After>1 M after
General self efficacy	8.3 (5.47)	8.5 (3.55)	8.0 (3.36)	n.s.	–	8.6 (4.62)	9.1 (4.31)	8.3 (4.47)	n.s.	–
Exercise self efficacy										
Physical fatigue	3.3 (1.15)	3.3 (1.22)	3.1 (1.31)	n.s.	–	2.9 (0.74)	3.5 (0.97)	3.2 (0.79)	n.s.	–
Mental stress	3.3 (1.22)	3.1 (1.16)	3.0 (1.28)	n.s.	–	2.6 (0.52)	3.3 (0.82)	3.0 (0.67)	**	∗Before<After
Busy	2.6 (1.16)	2.7 (1.07)	2.3 (1.29)	n.s.	–	2.4 (0.70)	2.7 (0.67)	2.4 (0.52)	n.s.	–
Vacation	3.6 (1.00)	3.6 (0.90)	3.4 (1.31)	n.s.	–	3.1 (0.88)	3.7 (0.48)	3.2 (0.92)	*	n.s.
Bad weather	3.5 (1.00)	3.6 (0.90)	3.3 (1.22)	n.s.	–	3.2 (0.79)	3.4 (0.97)	3.3 (0.82)	n.s.	–

***p<.01, *p<.05, Mean (SD)*

decrease in health protective behavior at 1M after the end of the program compared with immediately after intervention (MSe=3.00, $p<0.05$) and a significant increase in the <mental stress> component of exercise self-efficacy after intervention when compared to before intervention (MSe=2.87, $p<0.05$). No significant difference was seen in the <vacation> component of exercise self-efficacy.

DISCUSSION

In the present study, the mean number of steps per day before intervention was 4,890 in the TTM group and 4,717 in the control group. The mean number of steps per day for adult men in Japan according to the national health and nutrition survey was 7,575 [7], indicating that the mean for the present subjects was about 3,000 steps lower than the national average. This appears to result from the fact that most of the work done by the subjects involved sitting at a computer, that the subjects often worked overtime, and that most of subjects drove to the workplace because of a lack of convenient public transport. In addition, although many subjects set goals to walk during lunchtime or commute on foot instead of exercising during nonworking hours, intervention was affected by weather.

Under the present program, while the number of steps per day increased in the control group, it decreased at 1M after the end of the program. For the TTM group, the number of steps per day increased during lunchtime and commuting hours while on the program and remained high at 1M after the intervention ended, but this extended effect was not seen in the control group. These results suggested that individual guidance based on the TTM was effective in promoting long-term continuation of exercise habits gained during the program.

At present, increased physical activity in daily living is being closely examined as a means of preventing heart diseases, and in 1985 the Center for Disease Control (CDC) and the American College of Sports Medicine (ACSM) issued an important advisory: repeating low-intensity physical activities for a short period of time is a proper approach for promoting health [24]. Based on a finding that the same effects can be obtained by exercising for 30 min in one sitting or 10 min in three sittings [25], it is recommended that adults should perform moderate or higher physical activities for at least 30 min a day. The present study utilized a calorie counter as a tool to conveniently and objectively assess physical activity. The exercise program brought about changes in the number of steps per day, and the results showed increased physical activity and improved exercise adherence for the TTM group, thus suggesting the effectiveness of the TTM in promoting continuation of exercise.

For the TTM group, the health protective behavior score did not decrease until 1 after intervention, but for the control group, it decreased at 1M after intervention ended. This suggests that the TTM group was able to maintain high levels of health behavior to prevent diseases by being physically active, eating well, sleeping and resting sufficiently, and improving their surrounding environment. Therefore, in order to continue health protective behavior over the long-term it may be necessary to incorporate the TTM in programs to improve physical activities. Moreover, for the control group in this study, the exercise self-efficacy <mental stress> score after intervention was higher than that before intervention. For the TTM group, there was no marked change in the exercise self-efficacy score, possibly because the control group began exercising during a period of good weather, while the TTM group began exercising during a period in which frequently rained. While no marked changes were seen in exercise self-efficacy scores for the TTM group, the diurnal changes in the number of steps per day showed that the workers kept walking during lunchtime and commuting on foot during bad weather even 1M after the program ended. This suggests that the workers had gained confidence and therefore continued to exercise even in bad weather.

The important limitation of this study was that the small sample size did not allow for random distribution of subjects. We divided the subjects into two groups in this study according to their work situation at the company. This means that random distribution was not performed in this study. We must take this into consideration and exercise caution when evaluating the present results. In addition, the program was administered to the TTM group and the control group during different time periods, so the influence of seasonal and weather differences on physical activities cannot be ignored. Further study of this TTM based program for age, occupational type and program contents must be done on a larger scale with random distribution of subjects among workers at other small companies to confirm these findings.

While many studies have investigated the effects of general voluntary exercise programs in individuals at high concern for exercise [26,27], the present study is unique because an exercise program was administered to individuals that included subjects at low con-

cern for exercise. Moreover, the effects of the program were assessed not only before and after intervention, but also at 1M after the program ended, and we were able to investigate physical activity adherence and obtain clues for establishing an effective intervention technique for increasing and maintaining physical activities. Furthermore, the present study was meaningful because it was performed at a small-scale company with less than 50 employees, and these smaller companies are less likely to receive industrial health services. Moreover, the physical activity improvement program was adopted by the entire workforce.

ACKNOWLEDGMENTS: We are grateful to the workers who participated in the present study and the staff of the Tagawa regional occupational health center.

REFERENCES

1. Health and welfare statistics association. Annual statistical report of national health conditions, Health and welfare statistics association, Tokyo, Vol53, pp 298-303, 2006. (in Japanese)
2. Furuki K, Ashikaga K, Ishiwatari K, Hirata M, and Endo G. Investigative report on the present status of health management in small-scale companies. Occup Health J 2002; 25:21-28. (in Japanese)
3. Terada H, and Sone T. A study on effective implementation of the Shinjuku regional occupational health center program in Japan. J occup health 2000; 42:49-60. (in Japanese)
4. Naitou M, Iwamoto S, Shiwaku K, Kitajima K, Yamasaki M et al. Research on industrial health management and the regional occupational center for small-scale companies. Shimane Igaku 2004; 24:16-123. (in Japanese)
5. Ishii A. Yamano H, Takii H, Kizaki N, Nagatomi K et al. Evaluation of health intervention program after annual health check-ups in a small-scale company. J Kurume Med Assoc 2006; 63-70. (in Japanese)
6. Tatara K, Nakanishi N, and Fukuda H. Promotion of Healthy Japan 21. In: Healthy Japan 21 promotion guideline, ed. Tatara K, Gyosei, Tokyo, pp 2-58, 2001. (in Japanese)
7. Health and nutrition study group. Ministry of Health, Labour and Welfare. The national health and nutrition survey in Japan 2003. Dai-ichi Shuppan, Tokyo, pp 150-183, 2006. (in Japanese)
8. Oka K. Reliability and validity of the stages of change for exercise behavior scale among middle-aged adults. Jpn J Health Promotion 2003; 5:15-22. (in Japanese)
9. Prochaska JO, DiClemente CC, and Norcross JC. In search of how people change. Applications to addictive behaviors. Am Psychol 1992; 47:1102-1104.
10. Prochaska JO, Velicer WF, Rossi JS, Goldstein MG, Marcus BH et al. Stages of change and decisional balance for 12 problem behaviors. Health Psychol 1994; 13:39-46.
11. Marcus BH, and Simkin LR. The stage of exercise behavior. J Sports Med Phys Fitness 1993; 33:83-88.
12. Marcus BH, and Simkin LR. The transthoretical model: applications to exercise behavior. Med Sci Sports Exerc 1994; 26:1400-1404.
13. Oka K. Recent trends of research on exercise adherence utilizing the transtheoretical model of behavior change. Research journal of physical education 2000; 45:543-561. (in Japanese)
14. Shimomitsu T, Odagiri Y, Wakui S, Inoue S, and Takamiya T. Exercise behavior and psycho-behavioral factors : Cross-sectional study of change for exercise behavior. Descente Sports Sci 1999; 20:3-19. (in Japanese)
15. Resnick B, and Nigg C. Testing a theoretical model of exercise behavior for older adults. Nurs Res 2003; 52:80-88.
16. Nagano S. One-minute Exercise Diet. PHP Research Institute, Tokyo, pp 40-146, 2003. (in Japanese)
17. Inoue S, and Shimomitsu T. The behavioral approach to promote physical activity-application of the Transtheoretical Model-. In: Physical Activity and Lifestyle Related Diseases, Nipponrinsho, Osaka, pp 538-544, 2000. (in Japanese)
18. Ishii A, Toyomasu K, and Ishitake T. The evaluation of a fall prevention program in each stage of exercise behavior for the elderly. Health Sci 2004; 20:247-253. (in Japanese)
19. Munakata T. Health and disease seen from behavioral science, Medical-friend, Tokyo, pp 124-161, 1996. (in Japanese)
20. Bandura A. Self-efficacy: Toward a unifying theory of behavioral change. Psychol Rev 1977; 84:191-215.
21. Sakano Y. Verification of Validity of General Self-Efficacy Scale (GSES). Waseda studies in human sciences 1989; 2:91-98. (in Japanese)
22. Sakano Y, and Toujou M. The general self-efficacy scale. In: Handbook of psychological assessment, ed. I Agari, Nishimura Shoten, Niigata, pp 425-434, 1999. (in Japanese)
23. Oka K. Stages of change for exercise behavior and self-efficacy for exercise among middle-aged adults. Kosei kagaku Jpn J Public Health 2003; 50:208-215. (in Japanese)
24. Leon AS, Connett J, Jacobs DR Jr., and Rauramaa R. Leisure-time physical activity levels and risk of coronary heart disease and death. The multiple Risk Factor Intervention Trial. JAMA 1987; 258:2388-2395.
25. Pate RR, Pratt M, Blair SN, Haskell WL, Macera CA et al. Physical activity and public health. A recommendation from the Centers for Disease Control and Prevention and the American College of Sports Medicine. JAMA 1995; 273:402-407.
26. Takata Y, Nakanishi R, Isoda C, Nino M, and Maeda Y. The effect of a health promotion program at the worksite-An approach to Hyperlipoproteinemia in workers before middle age-. J occup health 2003; 45:43-49. (in Japanese)
27. Kohno H, Egawa K, Oida Y, Nagamatsu T, Kitabatake Y et al. Effect of functional fitness promotion program for community dwelling elderly persons using the transtheoretical model. Bulletin of the Physical Fitness Research Institute 2002; 100:11-20. (in Japanese)

Original Contribution

Kurume Medical Journal, 54, 9-24, 2007

Angiogenesis and Developmental Expression of Vascular Endothelial Growth Factor in Rat Lingual Papillae

TAKESHI HIRAO, TSUYOSHI SAGA*, JINGO KUSUKAWA AND KOH-ICHI YAMAKI*

Dental and Oral Medical Center, Department of Anatomy, Kurume University School of Medicine, Kurume 830-0011, Japan*

Received 30 October 2006, accepted 5 April 2007

Summary: We used an embryological approach to investigate development and microvasculature of lingual papillae, and expression of vascular endothelial growth factor (VEGF) in the rat tongue. Temporal changes in the rat tongue at each developmental stage from embryonic day 13 (E13) to postnatal day 7 (P7) were observed by intravascular injection of India ink and immunohistochemistry using a VEGF antibody. At E13, the primordium of circumvallate papilla was observed among various lingual papillae. VEGF was widely expressed at E16 on the proliferated epithelium and the connective tissue core of circumvallate papilla. Invasion by capillary sprouts forming the lingual papillae was observed at E17. The primordium of fungiform papillae was observed at E14. VEGF was strongly expressed around the basal cells of proliferated epithelial tissues of fungiform papillae at E17. At E18, blind-ended capillary sprouts invaded into connective tissue cores from subepithelial sinusoidal capillaries by sprout angiogenesis. At P1, the invading capillary sprouts formed loops by vascular remodeling. The primordium of foliate papillae was observed at E16. VEGF was slightly expressed, but uniformly at E17 on the epithelium, muscle cells, and fibroblasts of foliate papillae. At E18, vascular density was increased by angiogenesis. The primordium of filiform papillae was observed at E17. It was the last to develop among the lingual papillae. VEGF was expressed in the cytoplasm of grown epithelial cells of filiform papillae at E19, and in blind-ended capillary sprouts formed by angiogenesis in the connective tissue cores at E20. The capillary sprouts formed loops by vascular remodeling at P1. Consequently, VEGF was expressed on the papillary epithelium and connective tissue cores of papillae during development of the papillary epithelium, and invasion by capillary sprouts into each papillae was observed thereafter. These results suggest a close relationship between expression of VEGF and angiogenesis of lingual papillae in the rat.

Key words tongue, lingual papillae, angiogenesis, vascular endothelial growth factor (VEGF), immunohistochemistry

INTRODUCTION

The tongue has different functions including deglutition and mastication, and it also serves as an important information processing system controlling taste sensation. Morphological characteristics of the rat tongue have been described by various studies. It was reported that 4 types of lingual papillae: circumvallate papillae, fungiform papillae, foliate papillae, and filiform papillae exist in the dorsum of the tongue, and filiform papillae showed 3 morphological characteristics depending on regions on the lingual dorsum [1]. It is histologically known that taste buds form in circumvallate papillae, fungiform papillae, and foliate papillae,

Address for correspondence: Tsuyoshi Saga, Ph.D., Department of Anatomy, Kurume University School of Medicine, 67 Asahi-machi, Kurume 830-0011, Japan. Tel: +81-942-31-7540 Fax: +81-942-33-3233 E-mail: saga@med.kurume-u.ac.jp

Abbreviations: AP, anterior papillae; E, embryonic day; H/E, hematoxylin eosin staining; IE, interpapillary epithelium; P, postnatal day; PBS, phosphate buffered saline; PP, posterior papillae; VEGF, vascular endothelial growth factor; VPF, vascular permeability factor.

but not in the 3 types of filiform papillae which have their own specific differentiated epithelia. Although there are slight differences in the classification of the 3 types of filiform papillae depending on observers, they are classified into simple conical papillae, giant conical papillae, and branched papillae [2,3]. Many researchers reported on development of papillae [4-9], but no study has been performed to simultaneously observe development and angiogenesis of lingual papillae. A detailed study of the vascular morphology of lingual papillae in the adult rat was reported with respect to the vascular system [2,3,10], but angiogenesis of lingual papillae has not been observed except for that of filiform papillae [11].

It is generally known that angiogenesis plays an important role in the early embryonic stages of organs [12-15]. Vascular endothelial growth factor (VEGF) is a cytokine which plays a leading role in angiogenesis. VEGF was initially discovered as a vascular permeability factor (VPF) [16]. Then, a heparin-binding growth factor that acts specifically on endothelial cells was discovered, and was named as VEGF [17]. It was later clarified that VEGF and VPF were the same glycoprotein, and is currently considered as one of the most potent angiogenetic factors having both a growing effect on endothelial cells and a vascular hyperpermeability effect. VEGF is secreted according to oxygen and nutritional requirements of tissues or cells [18-21]. VEGF is expressed in many organs and tissues during the embryonic period, as well as in cancerous cells showing strong proliferation [22-24]. VEGF family has been expanded by the isolation of four additional growth factors, VEGF-B, -C, -D, and -E. In this study, the expression of the VEGF namely VEGF-A which is the most powerful angiogenic factor in early development is investigated. Moreover, five isoforms of VEGF (-A) exist due to differential splicing of a single gene: $VEGF_{121}$, $VEGF_{145}$, $VEGF_{165}$, $VEGF_{189}$, and $VEGF_{206}$. Of these, $VEGF_{121}$ and $VEGF_{165}$ are secreted soluble glycoproteins and $VEGF_{165}$ is the most abundant VEGF. In this study, we examined by using the VEGF antibody that mainly react with the $VEGF_{165}$ [25,26].

We histologically observed morphogenetic processes of lingual papillae using rat fetuses and newborn rats; and in particular, we investigated the development of microvasculature of lingual papillae using the Indian ink injection method. In addition, we investigated $VEGF_{165}$ expression in lingual papillae of the growing rat using immunohistochemistry to clarify the role of VEGF in lingual papillae angiogenesis.

MATERIALS AND METHODS

Animals

Study protocols have been approved by the Committee on Animal Experimentation, Kurume University. Female Wistar rats after mating were raised at the Kurume University center as experimental animals, and the fetuses and newborn rats from maternal animals, and adult rats were used. Mating was confirmed by the presence of a vaginal plug, and embryonic stages were calculated by considering animals with a plug as the first embryonic day (E1). Tongues to be examined in this study were removed from embryos from E13 to E21, and the first postnatal day (P1) to P7, and from 8 adult rats.

Preparation of specimens

Preparation of specimens for histological observation

Heads of fetuses and newborn rats were dissected, and were immediately immersed and fixed in Bouin solution. Following fixation, specimens were prepared using the entire head of animals from E13 to E18, and the isolated tongue alone of animals from E19 to P7. Tissues were embedded in paraffin according to conventional methods. Tongue specimens of adult rats were prepared by isolating the tongue alone. These were fixed and embedded in the same manner. Then, 8 to 15-μm serial sections were cut sagittally, and frontal and horizontal sections were used for staining.

***Hematoxylin/eosin (H/E) staining*:** Paraffin sections were stained with H/E, using conventional methods, and morphologies of the tongue and lingual papillae of adult rats and embryonic specimens were observed by light microscopy.

***Immunohistochemistry*:** Immunohistochemistry was performed for tongue paraffin sections of each embryonic stage using a VEGF antibody as primary antibody. Following deparaffinization, each section was incubated with 0.3% hydrogen peroxide solution to inactivate endogenous peroxidase activity, and was reacted for 60 min with 10% normal rabbit serum to block non-specific binding sites for the secondary antibody. Anti-VEGF goat polyclonal IgG (SANTA CRUZ, CALIFORNIA, USA) was used as primary antibody, and biotinylated anti-goat rabbit-IgG (NICHIREI, TOKYO, Japan) was used as secondary antibody. Peroxidase-conjugated streptavidin (NICHIREI, TOKYO, Japan) was used as the enzymatic reagent, and 3,3′-diaminobenzidine tetrahydrochloride in 50 mM Tris-HCl buffer (pH 7.6) containing 0.003% hydrogen peroxide was used for

visualization of the final reacting products. This anti-VEGF antibody reacts with the 165, 189 and 121 amino acid splice variants of VEGF of mouse and rat origin (SANTA CRUZ, CALIFORNIA, USA). To confirm specificity of immunocytochemical staining, the primary antiserum was replaced by phosphate buffered saline (PBS).

Preparation of microvascular specimens

***Injection of Indian ink*:** Before injection of Indian ink, 99% diethyl ether was aspirated in rat fetuses and newborn rats, and animals were fixed in the supine position under general anesthesia. Following thoracotomy, the heart was injected with physiological saline at 37°C, and was fully perfused until blood in the tongue vessels was eliminated. Then, Indian ink solution at 37°C in 10% gelatin was immediately injected within 2 to 3 min using hand pressure of 100-120 mmHg [27]. After confirmation of black coloration of the dorsum of the tongue by Indian ink injection, the specimens were immediately cooled to coagulate gelatin, and were further fixed with 10% formaldehyde solution.

***Celloidin embedding and observations*:** The tongue was isolated after fixing the specimens for 2 days in 10% formaldehyde solution, dehydrated with alcohol, and embedded with celloidin. Using prepared Indian ink-injected microvascular specimens at each stage, the tongue surface was observed using stereoscopic microscopy. Serial 60-μm thick sagittal sections were prepared, and angiogenesis of the tongue and lingual papillae at each embryonic stage was observed using frontal and horizontal sections and light microscopy.

RESULTS

Morphology of the tongue and lingual papillae in the adult rat

Macroscopic observations

The tongue of adult rat is divided into 3 areas: the apex which is the tip of the tongue, the body which covers the area from the apex of the tongue to the circumvallate papillae, and the root which is the posterior area of the circumvallate papillae. Situated at the center of the body of the tongue is the intermolar eminence with a side view protrusion dividing the body of the tongue into anterior and posterior regions. On the midline of the dorsum of the tongue from the apex of the tongue to the center of the body of the tongue is the median lingual sulcus.

There are 4 types of lingual papillae on the dorsum of the tongue in adult rat, similarly to the human tongue: circumvallate papillae, fungiform papillae, foliate papillae, and filiform papillae. In the rat, filiform papillae are further classified into 3 subtypes (simple conical papillae, giant conical papillae, and branched papillae) with different morphologies depending on their location on the dorsum of the tongue. The simple conical papillae and the fungiform papillae are located on the anterior region of the tongue. Cone shaped simple conical papillae possess tongue-like processes at the tip, and the processes are sloped backward toward the direction of the root of the tongue, and are found in dense numbers from the apex of the tongue to the anterior region of the tongue. Low and round fungiform papillae are sporadically observed among simple conical papillae. Giant conical papillae are observed in dense numbers in the limited crescent region on the intermolar eminence. They are bigger than simple conical papillae in both thickness and height, and the tongue-like processes at the tip are slanted forward in the direction of the apex of the tongue. In the posterior region of the tongue, branched papillae, foliate papillae, and circumvallate papillae are well distributed. Branched papillae are observed in dense numbers in the posterior region of the tongue from the back of giant conical papillae to the front of circumvallate papillae, and the tip of tongue-like processes is forked into several branches, and slanted in the direction of the body of the tongue. Five to 6 foliate papillae separated by several vertical furrows are observed at the lingual side of the posterior region of tongue. One oval-shaped circumvallate papilla was observed at the most poste-

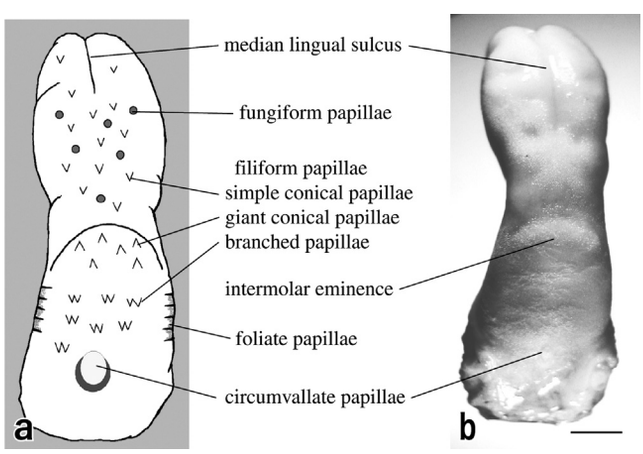


Fig. 1. Macroscopic observation of adult rat tongue. **a:** Schematic diagram in adult rat, each lingual papilla is shown. **b:** Photograph of adult rat tongue. (—= 3 mm)

rior midline of the posterior region of the tongue, and there were no lingual papillae in the root of the tongue behind the circumvallate papilla (Figs. 1a, b).

Light microscopical observation of lingual papillae

Morphology of lingual papillae in adult rat was observed by light microscopy. Lingual papillae generally consisted of epithelial and connective tissues. Epithelial tissues are stratified squamous epithelium with a keratinized layer observed on the utmost surface layer. Connective tissues are abundant with fibroblasts and blood vessels, and the connective tissue core is formed by expansion. Connective tissues just under the apical papillary epithelium form a rolling shape, and secondary papillae are formed at the top of connective tissue core.

***Circumvallate papillae*:** Circumvallate papillae are single, large, oval papillae with a longitudinal diameter of approximately 700 μm, and a width of approximately 600 μm. They were surrounded by a U-shaped furrow of approximately 400 μm in depth, which lacks a front portion. Epithelial tissues on the dorsum of the tongue of circumvallate papillae consist of several layers of stratified squamous epithelium. There is a thin keratinized layer on the utmost surface layer, and rolling secondary papillae form at the top of the connective tissue core. There are numerous bell-shaped taste buds in the lateral epithelium facing the depressed furrows, and serous glands are observed in connective tissues at the bottom of the furrows (Figs. 2a-c).

***Fungiform papillae*:** Fungiform papillae are sea anemone-like protrusions approximately 150 μm in diameter and 180 μm in height, from the epithelial basal layer with a small depression on the top. There were numerous fungiform papillae in the anterior dorsum region of the tongue. Epithelial tissues were thin, and lack a keratinized layer, and there was one bell-shaped taste bud in the epithelium depressed at the center. Secondary papillae formed at the top of the connective tissue core (Fig. 2d).

***Foliate papillae*:** On both sides of the lingual margins of the posterior region of the tongue, we observed foliate papillae which extended between several furrows of depressed epithelium. Of the 5 to 6 foliate papillae on each side, the most posterior was the biggest in size (approximately 200 μm in both width and furrow depth). Epithelial tissues of foliate papillae facing the dorsum of the tongue were made of several layers of stratified squamous epithelium, possessing a thin keratinized layer on the utmost surface, and rolling secondary papillae formed at the top of connective tissue cores. In the lateral epithelium facing the depressed furrows were a few bell-shaped taste buds, and serous glands were observed in the connective tissue just below the furrows (Fig. 2e).

***Filiform papillae*:** Three types of epithelial tissues (anterior papillae (AP), posterior papillae (PP), and interpapillary epithelium (IE)) with specific differentiation patterns characterized the 3 types of filiform papillae (simple conical papillae, giant conical papillae, and branched papillae) (Figs. 2f-g). Cone shaped simple conical papillae of the anterior region of the tongue were approximately 100 μm in height and 50 μm in basal diameter, and their tips were bent backward toward the root of the tongue. The anterior part of papillae consisted of a granular layer containing numerous keratohyalin granules in the cytoplasm, which were strongly stained by eosin whereas the keratinized layer was uniformly and lightly stained by eosin. There was no keratohyalin granule in the posterior part of papillae, and layers of squamous cells with small nuclei stained by eosin were observed in the keratinized layer. Numbers of keratohyalin granules with different sizes increased from the middle to upper layer of epithelial tissues of the interpapillary epithelium. The keratinized layer was strongly stained in a rolling manner, and neither nuclei nor keratohyalin granules were observed (Fig. 2f). The shape of the giant conical papillae on the intermolar eminence was similar to that of simple conical papillae, but the former were thicker and taller than the latter, and the tongue-like processes were slanted forward compared to those in the simple conical papillae. In giant conical papillae, a granular layer was observed in the posterior part but not in the anterior part of papillae. The interpapillary epithelium was narrower than the epithelium of simple conical papillae, and fewer keratohyalin granules were present on the upper layer of epithelial tissues (Fig. 2g). Tongue-like processes of branched papillae of the posterior region of the tongue were branched to form several tips which were slanted toward the root of the tongue. Similarly to the simple conical papillae, a granular layer was observed in the anterior part, but not on the posterior part of papillae. The interpapillary epithelium was very narrow and a few small keratohyalin granules were observed (Fig. 2h).

Morphogeneses of the tongue and lingual papillae, and expression of VEGF

Lingual tissue differentiation and development of lingual papillae

Mandibular processes and lateral lingual swellings were not clearly distinguished at E13, and the epithelial transition was smooth (Fig. 3a). At this stage, flat

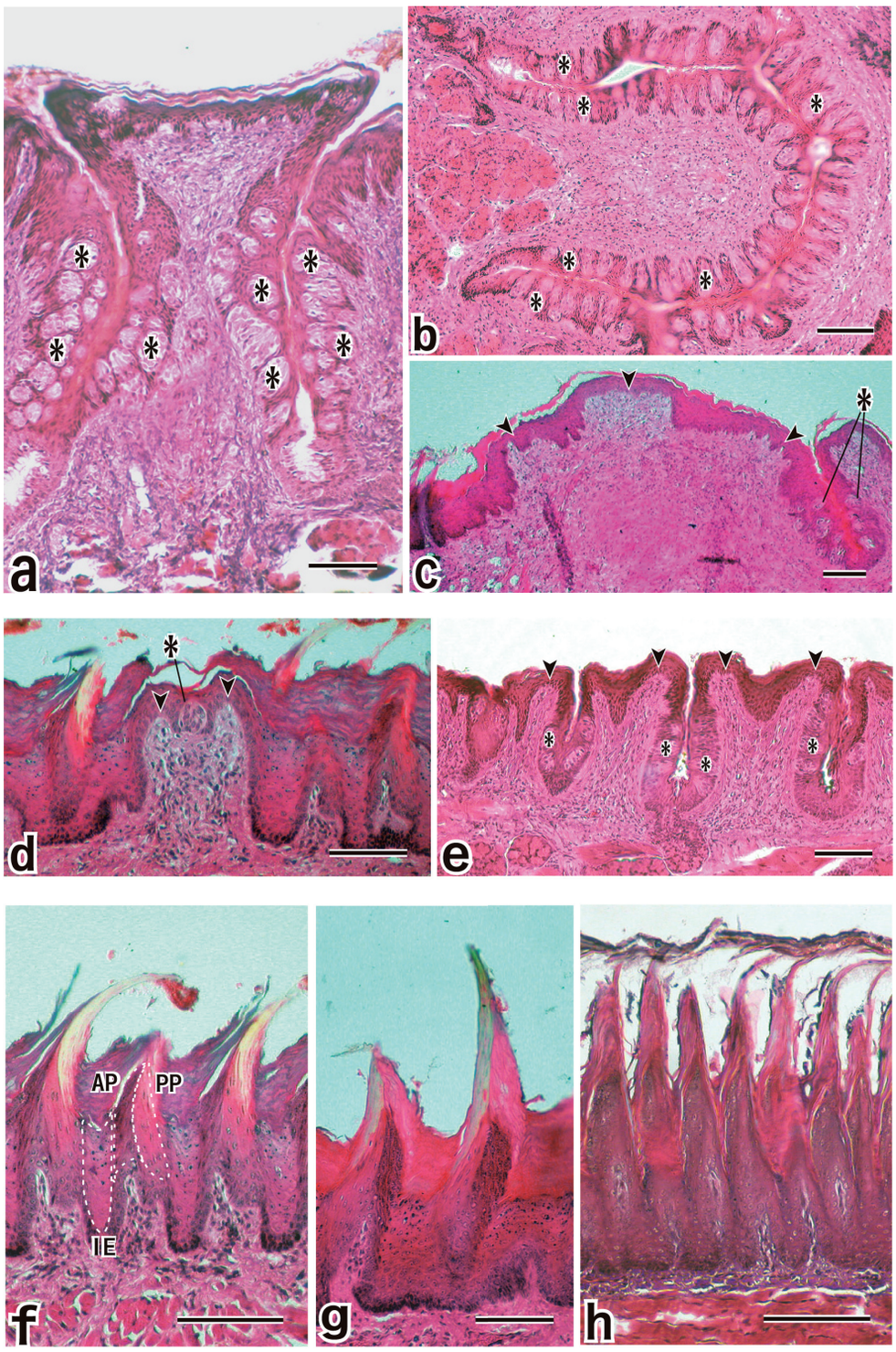


Fig. 2. H/E staining of each lingual papilla in adult rat. **a:** Frontal section of the posterior region of circumvallate papilla. Many taste buds (∗) exist on the lateral epithelium. **b:** Horizontal section of middle part of circumvallate papilla. **c:** Mid sagittal section of circumvallate papilla. **d:** Sagittal section of fungiform papillae. **e:** Horizontal section of foliate papillae. **f-h:** Sagittal sections of three kinds of filiform papillae. **f:** Simple conical papillae. Apparent three types of epithelial tissues are distinguished. **g:** Giant conical papillae. **h:** Branched papillae. **AP:** Anterior papillae. **IE:** Interpapillary epithelium. **PP:** Posterior papillae. ▼: Secondary papillae. ∗: Taste bud. (— = 100 μm)

endothelial cells were observed in the mesenchymal tissue at the bottom of the root of the tongue, whereas aggregates of cells linked together were observed in the subepithelium of the anterior tongue. Oval cells were observed in peripheral aggregates, whereas nucleated round cells were observed in central aggregates (Fig. 3f). The primordium of circumvallate papillae with a slightly depressed lingual surface was observed on the anterior root of the tongue. The epithelium of circumvallate papillae was slightly proliferated, and showed a smooth transition to the surrounding epithelium (Fig. 3a).

At E14, basic morphology of the tongue was established, and the mandible and the tongue were distinguishable (Fig. 3b). The primordium of fungiform papillae with a slight extension at the basement membrane side of the epithelium was observed on the dorsum of the anterior tongue, from the apex to the body of the tongue (Fig. 3g). Subepithelial endothelial cells still showed an immature oval shape, and blood cells were nucleated and undifferentiated.

At E15, mandibular processes were further developed, and Meckel's cartilage was observed within them. Mesenchymal lingual tissues became spindle or star shaped, and accumulated at the center of the tongue to show a regular myoid arrangement (Fig. 3c). There were no significant changes in thickness of epithelial tissues in the dorsum of the tongue, but epithelial cells had proliferated even on the surface layer, and were not in contact with the basement membrane. The epithelium of circumvallate papillae was still slightly depressed, and had proliferated giving rise to 5 to 6 layers (Fig. 3h). Flat endothelial cells were observed subepithelially, but blood cells were still nucleated and undifferentiated.

At E16, the nasal and oral cavities were separated by lateral palatine processes, and the tongue moved down. Differentiation of mesenchymal tissues into the transverse lingual muscle, superior longitudinal lingual muscle, and vertical lingual muscle was observed, and specific arrangements of muscle tissues became notable. Morphology of the tongue resembled that of the adult rat, and the intermolar eminence was observed (Fig. 3d). Epithelial tissues depressed under connective tissues at the lingual margin of the posterior region of the tongue, and the primordium of foliate papillae could be seen (Fig. 3i). Subepithelial endothelial cells had proliferated, differentiation of blood cells was advanced, and numerous denucleated blood cells were observed.

At E17, epithelial tissues, muscle tissues, and vascular systems were further differentiated, and their morphologies resembled those in adult rat (Fig. 3e). Numerous primordia of filiform papillae were observed on the basement membrane of epithelial tissues which had proliferated to reach 4 to 5 layers on the dorsum of the tongue from the apex of the tongue to the body of the tongue (Fig. 3j). All 4 types of lingual papillae were observed after development of filiform papillae, but epithelial keratinization characteristic of lingual papillae or taste buds was still not observed. Mesenchymal cells accumulated around blood vessels running between muscle tissues, and were ready to differentiate into mural cells.

From E18 to E19, epithelial tissues of the dorsum of the tongue rapidly grew to form 5 to 6 layers. Smooth muscles surrounding blood vessels running between muscle tissues, and differentiation of mural cells were observed. At E20, epithelial tissues on the dorsum of the tongue were keratinized, and blood vessels surrounding muscle tissues matured with an expanding vascular lumen. At E21, morphology of the tongue mostly resembled that in adult rat.

Morphogenesis of each lingual papilla: expression of VEGF and angiogenesis

***Circumvallate papillae*:** Following development of the primordium of circumvallat papilla with a slightly depressed epithelium at E13, epithelial tissues thickened further at E15 (Figs. 3a, h). At E16, epithelial tissues at the posterior part of circumvallate papilla were further depressed in connective tissues, and the connective tissue core at the anterior part of circumvallate papilla became thickened, and expanded. Fibroblast proliferation was observed on the expanding connective tissue core, and VEGF was widely expressed on the thickened epithelium and expanded connective tissue core (Figs. 4a, b). There was no capillary sprout invading the expanding connective tissue core at this stage (Fig. 4c). At E17, the connective tissue core was extended at the anterior part of circumvallate papilla, capillary sprouts invaded into the connective tissue core (Figs. 4d, e). From E19 to E21, furrows made by depressed epithelium became more evident, and morphology of circumvallate papilla was similar to that in adult rat. At P1, taste buds were confirmed in the lateral epithelial tissues of the furrows, and blood vessels developed (Figs. 4f, g). At P7, differentiation of circumvallate papillary epithelium had progressed, with increasing number and size of taste buds observed in the lateral epithelium of furrows, and blood vessels that formed papilla were further grown (Figs. 4h, i).

***Fungiform papillae*:** Following development of the

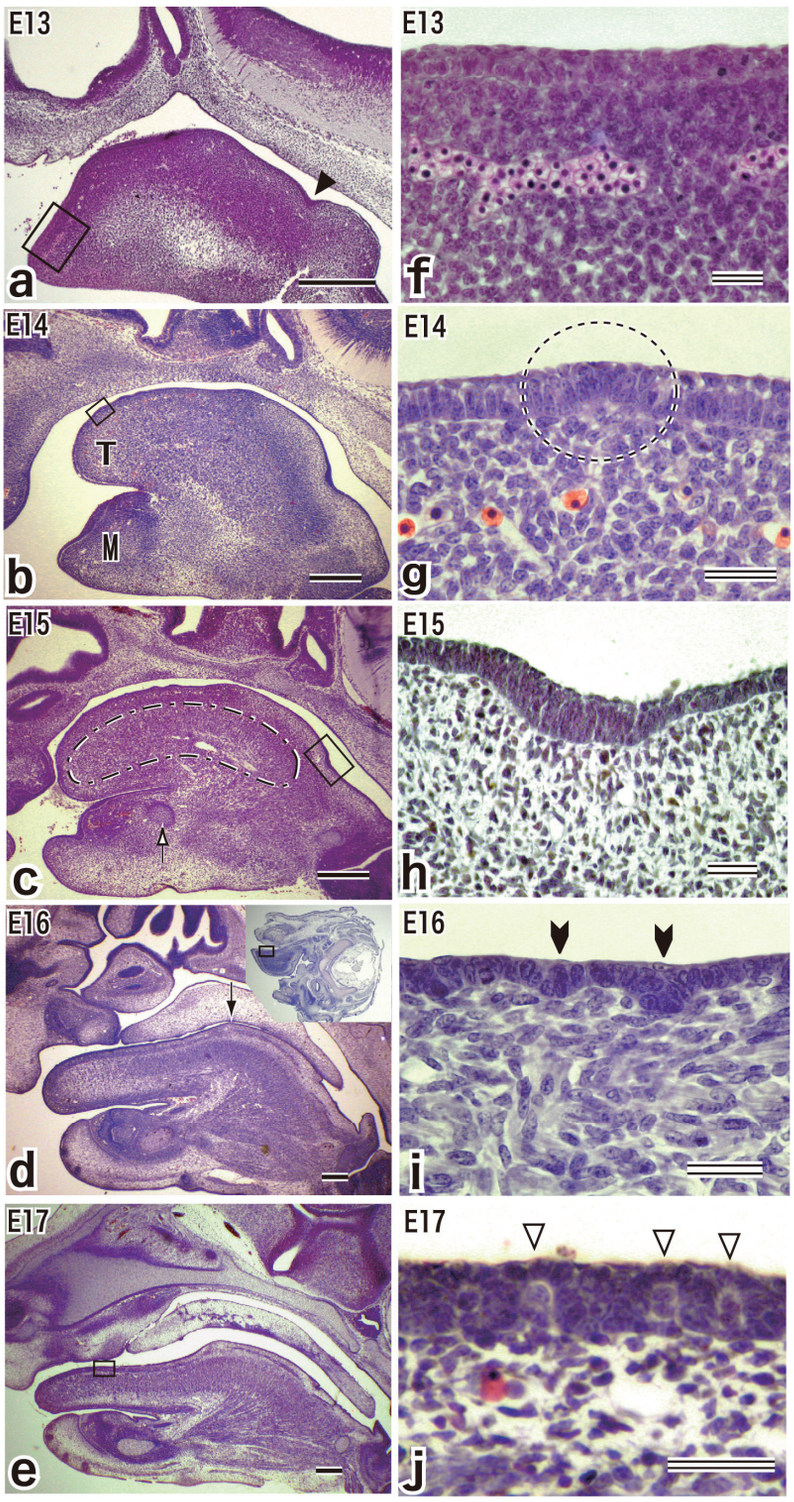


Fig. 3. Morphogenesis of the tongue and lingual papillae at E13, E14, E15, E16, and E17. **a-e:** Sagittal section through oral cavity at each stage. **f-j**: Magnified views of a-e (□). **a:** Tongue and mandibular processes are not clearly distinguished. Primordium of circumvallate papilla (▼) was observed. **f:** Anterior part of the tongue primordium. **b:** Tongue (T) and mandibular process (M) are distinguishable. **g:** Primordium of fungiform papillae (◌) on the dorsum of the tongue at E14. **c:** Meckel's cartilage (⍋) was observed within developed mandibular processes, and a regular myoid arrangement (◠) was developed in the tongue. h: Epithelium of circumvallate papilla proliferated. **d:** Intermolar eminence (↓) is observed in developed tongue. An additional right upper photomicrograph is horizontal section of rat head. **i:** Side margin of the posterior region of the tongue. Primordiums of foliate papillae (⩛) are distinguished. **e:** Well developed tongue like as in adult. **j:** Anterior part of the dorsum of the tongue at E17. Some primordiums of filiform papillae (▽) are observed. (═ = 30 μm, — = 300 μm).

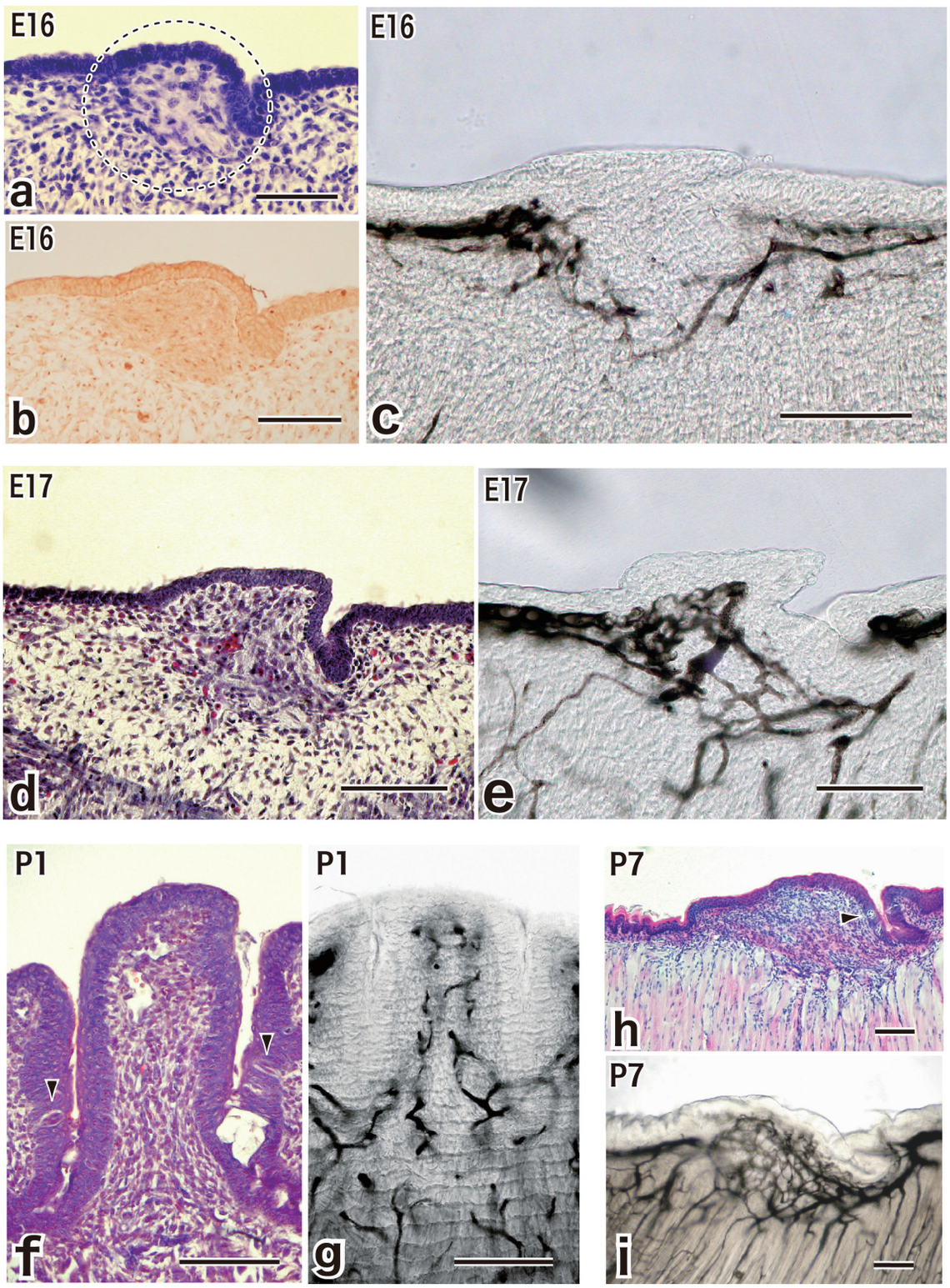


Fig. 4. Photomicrographs of circumvallate papilla at E16, E17, P1, and P7. **a-c:** Sagittal sections of circumvallate papilla at E16. **a:** Primordium of circumvallate papilla is shown as ◌. H/E staining. **b:** VEGF immunoreactivity was widely expressed on the thickened epithelium and expanded connective tissue core. **c:** No capillary sprouts observe in the expanding connective tissue core. India ink injection. **d** and **e:** Sagittal sections of circumvallate papilla at E17. **d:** Circumvallate papilla slightly grows. H/E staining. **e:** Capillary sprouts invade into the connective tissue core. India ink injection. **f** and **g:** Frontal sections of circumvallate papilla at P1. **f:** Taste buds (▼) are differentiated in the lateral epithelial tissues of the circumvallate papilla. H/E staining. **g:** India ink injection. **h** and **i:** Sagittal sections of circumvallate papilla at P7. **h:** Circumvallate papilla is developed like an adult. H/E staining. **i:** Well developed blood vessels observe. India ink injection. (— = 100 μm)

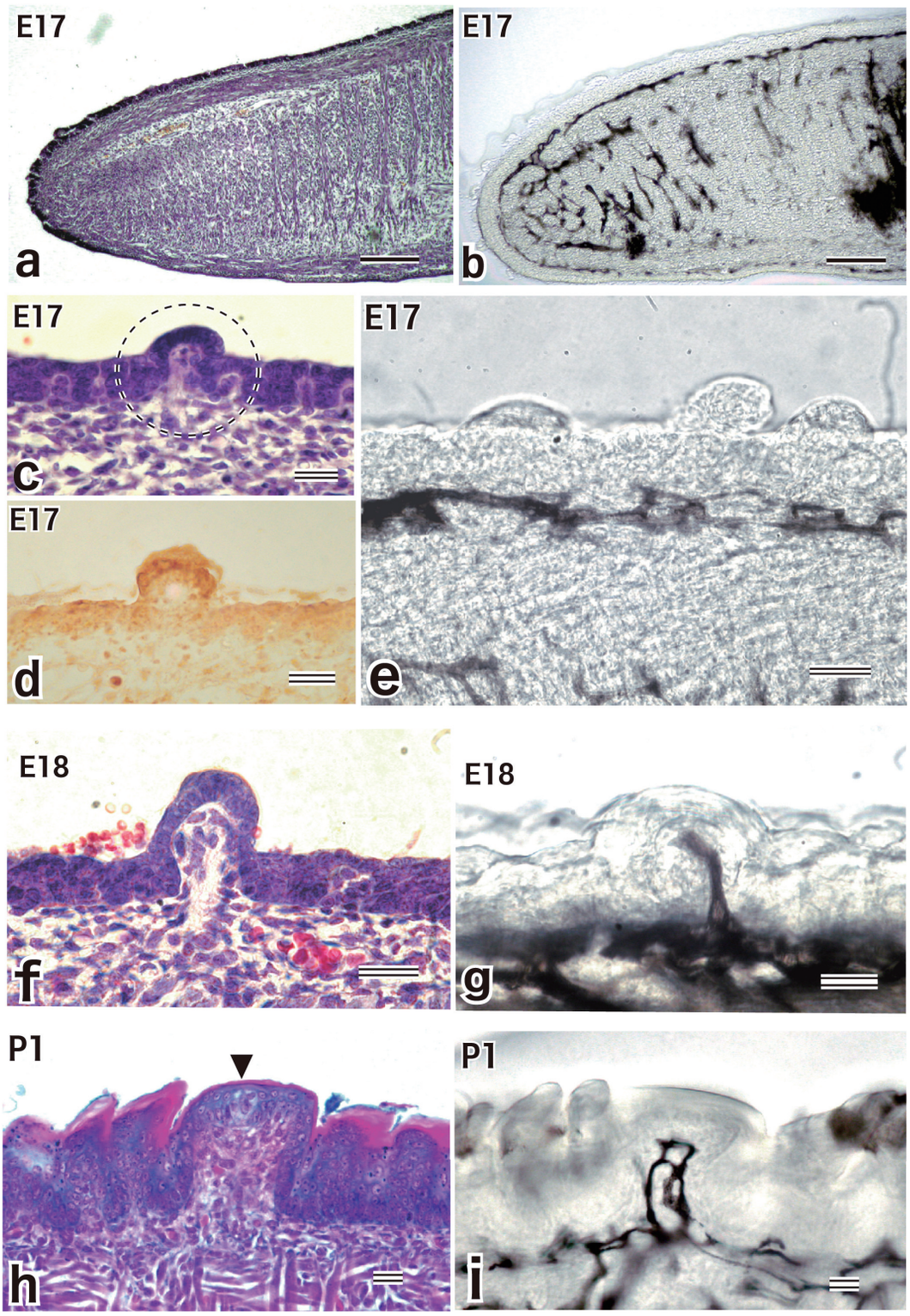


Fig. 5. Photomicrographs of sagittal sections of fungiform papillae at E17, E18 and P1. **a** and **b:** Anterior region of the tongue at E17. **a:** Lingual muscle are differentiated. H/E staining. **b:** Blood vessels between muscle tissues develop. India ink injection. **c-e**: Fungiform papillae at E17. **c:** Primordium of fungiform papilla is shown as ◌. H/E staining. **d:** VEGF immunoreactivities are demonstrated around the basal cells of proliferated epithelial tissues. **e:** No capillary sprouts observe in the connective tissue core of fungiform papillae primordium. India ink injection. **f** and **g:** Fungiform papilla at E18. **f:** Fungiform papilla is growing. H/E staining. **g:** Blind-ended capillary sprout invades in the connective tissue core. India ink injection. **h** and **i:** Fungiform papilla at P1. **h:** Fungiform papilla form like an adult. A taste bud (▼) is differentiated at the top of the fungiform papilla. H/E staining. **i:** Capillary sprout grows to reveal a loop shape. India ink injection. (═ = 20 μm, — = 200 μm)

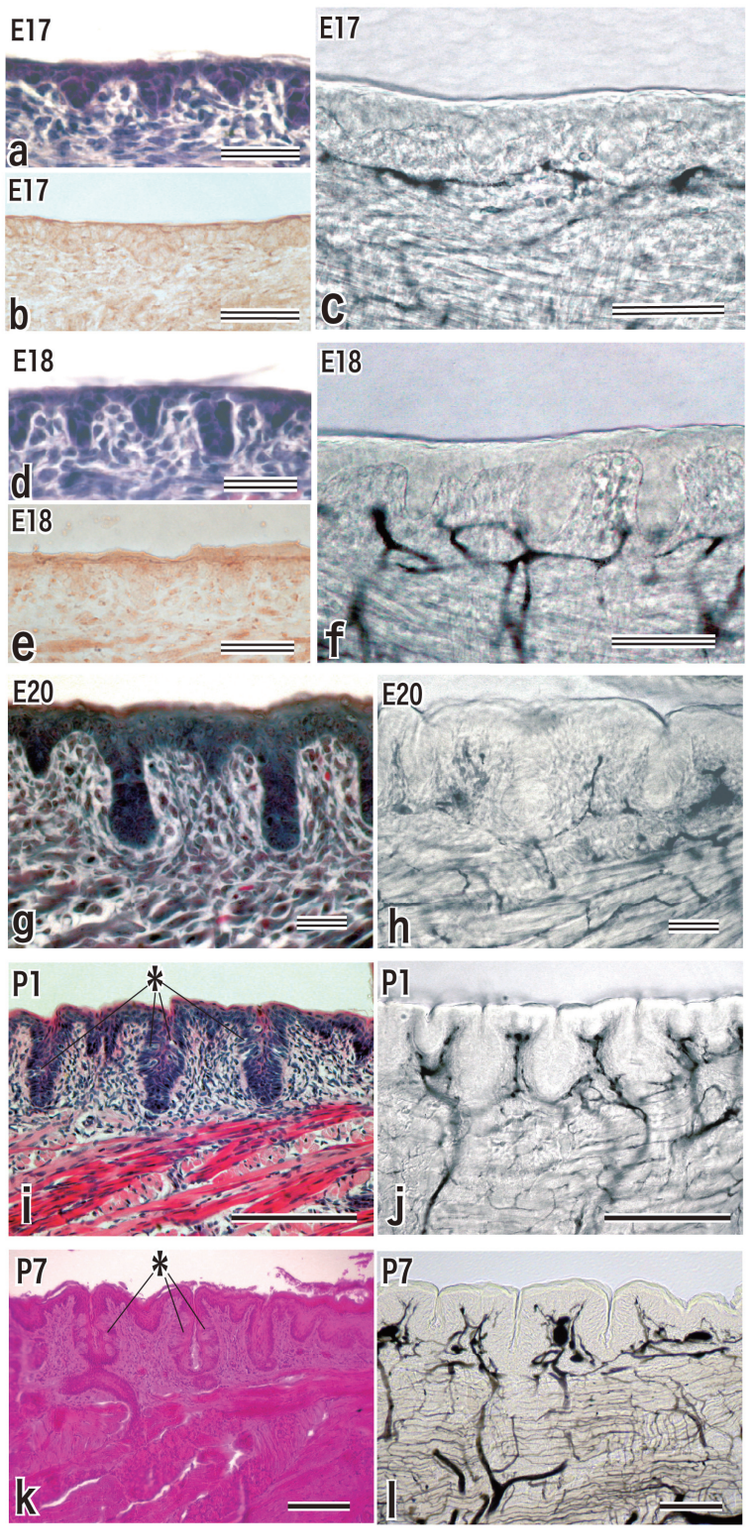


Fig. 6. Photomicrographs of horizontal sections of foliate papillae at E17 (**a-c**), E18 (**d-f**), E20 (**g** and **h**), P1 (**i** and **j**), and P7 (**k** and **l**). **a:** Slightly developed primordiums of foliate papillae. H/E staining. **b:** No apparent VEGF immunoreactivities. **c:** Linear and thin blood vessels are observed. India ink injection. **d:** Proper mucous membrane of foliate papillae become thicker. H/E staining. **e:** VEGF immunoreactivity appear in the vicinity of the epithelial basement membrane. **f:** Blood vessels protrude toward the epithelium in a loop shape. India ink injection. **g:** Epithelium and secondary papillae are developed. H/E staining. **h:** Blood vessels are widely observed. India ink injection. **i:** Taste buds (∗) were observed in the lateral epithelium. H/E staining. **j:** Blood vessels increase density in the connective tissue core. India ink injection. **k:** Foliate papillae forms like an adult. H/E staining. **l:** Well developed blood vessels in the foliate papillae. India ink injection. (═ = 30 μm, — = 150 μm)

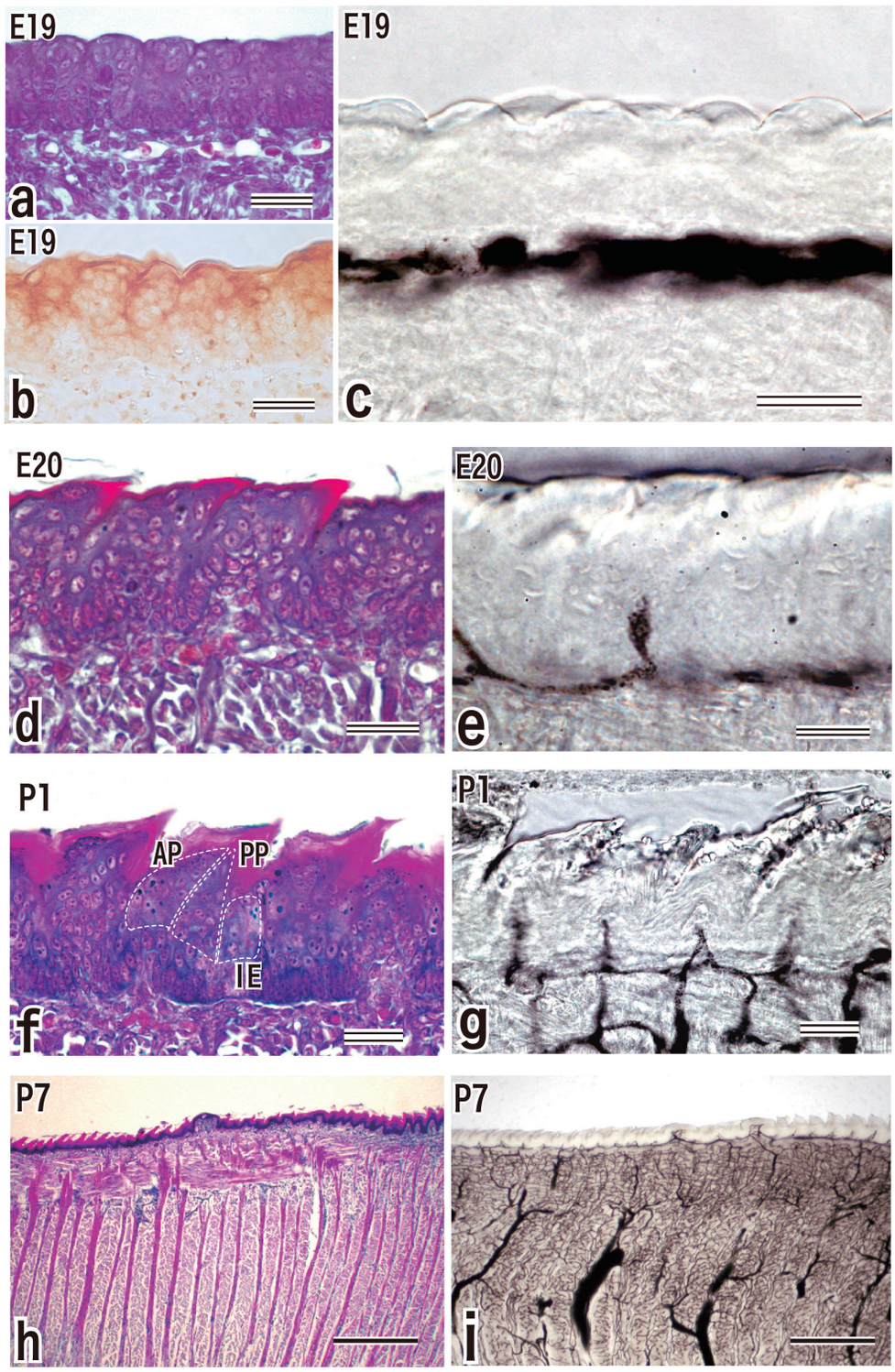


Fig. 7. Photomicrographs of sagittal sections of filiform papillae at E19 (**a-c**), E20 (**d** and **e**), P1 (**f** and **g**), and P7 (**h** and **j**). **a:** Slightly developed primordiums of filiform papillae. H/E staining. **b:** VEGF Immunoreactivities observe in the epithelial layer. **c:** No capillary sprouts invade into connective tissue cores. India ink injection. **d:** Slightly differentiated filiform papillae. A keratinized layer stained with eosin differentiates on the surface of epithelial layer. H/E staining. **e:** Blind-ended capillary sprouts are observed. India ink injection. **f:** Three types of epithelia anterior papillae (**AP**), posterior papillae (**PP**), and interpapillary epithelium (**IE**) are differentiated. H/E staining. **g:** Capillary sprouts become loop shaped. India ink injection. **h:** Well developed filiform papillae. H/E staining. **i:** Well developed blood vessels in the filiform papillae. India ink injection. (═ = 30 μm, — = 300 μm)

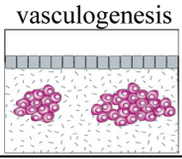
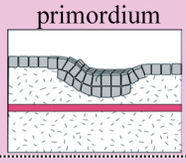
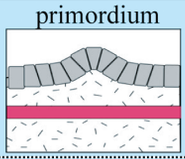
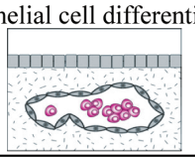
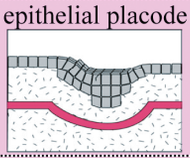
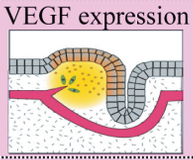
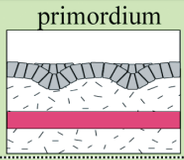
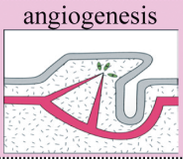
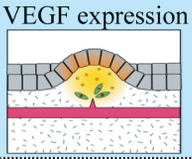
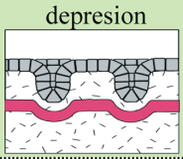
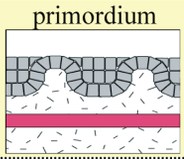
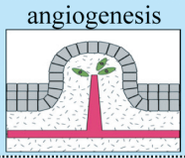
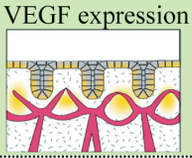
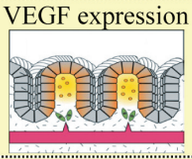
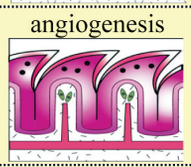
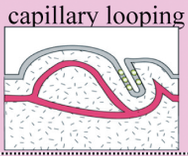
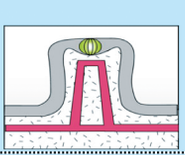
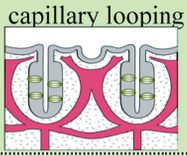
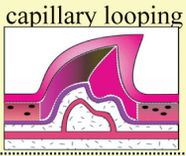
stage	tongue	circumvallate papillae	fungiform papillae	foliate papillae	filiform papillae
E13	vasculogenesis 	primordium 			
E14	tongue differentiation		primordium 		
E15	endothelial cell differentiation 	epithelial placode 			
E16	lingual muscle differentiation blood cell denucleation	VEGF expression 		primordium 	
E17	capillary plexus formation	angiogenesis 	VEGF expression 	depresion 	primordium 
E18		vascular remodeling	angiogenesis 	VEGF expression 	
E19	epithelial thickening vascular myogenesis		vascular remodeling	angiogenesis	VEGF expression 
E20	epithelial keratinization			Microvascular density increase	angiogenesis 
E21					vascular remodeling
P1		taste bud serous gland capillary looping 	taste bud capillary looping 	taste bud serous gland capillary looping 	epithelial differentiation capillary looping 
P7	well developed	well developed	well developed	well developed	well developed

Fig. 8. Lingual development, in particular, angiogenesis and expression of VEGF from E13 to P7.

primordium of fungiform papillae at E14 (Fig. 3g), a dome shaped expansion became pronounced at E17. At this stage, each lingual muscle was differentiated, and a specific arrangement with regards to lingual muscles became evident. Blood vessels between muscle tissues developed rapidly, and we observed dense sinusoidal capillaries in the subepithelium (Figs. 5a, b). A distinct dome shaped expansion of fungiform papillae was seen with epithelial proliferation and expansion of the connective tissue core (Fig. 5c). VEGF was expressed around the basal cells of proliferated epithelial tissues (Fig. 5d). Capillary sprouts that had invaded into the connective tissue core from the subepithelial sinusoidal capillaries were not observed at E17 (Fig. 5e). At E18, fungiform papillae were observed as bigger dome shaped eminences, and invasion by blind-ended capillary sprouts and protrusion of the connective tissue core were observed in fungiform papillae (Figs. 5f, g). From E19 to E21, fungiform papillae were observed as low, flat, dome-shaped eminences scattered among filiform papillae, while one taste bud was confirmed at the center of the epithelium facing the dorsum of the tongue at P1, and the capillary sprouts of fungiform papillae grew to reveal a loop shape (Figs. 5h, i).

***Foliate papillae*:** Following development of the primordium at E16 (Fig. 3i), epithelial tissues on upper papillae became thin with 1 to 2 layers at E17, and epithelial depressions of 3 to 4 layers were observed in connective tissues. However, localization of VEGF immunoreactivity was not obvious at this stage (Figs. 6a, b). The proper mucous membrane between the epithelium and muscle layers was thin, with 7 to 8 layers, but linear and thin blood vessels were observed in a horizontal direction (Fig. 6c). At E18, the basal epithelium was further depressed, and an epithelial cell layer of 5 to 6 layers was observed. The proper mucous membrane which was equivalent to connective tissues also became thicker. VEGF localization was not evident, and it was expressed weakly and uniformly on the epithelial cell layer, muscle cells, and fibroblasts. Strong VEGF expression was observed only in the vicinity of the epithelial basement membrane (Figs. 6d, e). Blood vessels of the proper mucous membrane protruded toward the epithelium in a loop shape (Fig. 6f). At E20, epithelial cells of foliate papillae had grown, M-shaped secondary papillae had developed on the basal layer, and a thin keratinized layer had developed on the utmost surface of the epithelium. Epithelial tissues were further depressed toward connective tissues (Fig. 6g). Blood vessels were widely observed in the proper mucous membrane from the subepithelium to the muscle layer (Fig. 6h). At P1, serous gland cells densely stained by hematoxylin were observed in connective tissues under the bottom furrows. Taste buds were observed in the lateral epithelium of furrows, and blood vessels observed in the connective tissue core had developed with increasing density (Figs. 6i, j). At P7, differentiation of the papillary epithelium consisting of foliate papillae was advanced, and numerous taste buds in the lateral epithelium and enlarged vascular lumens in the connective tissue core were observed (Figs. 6k, l).

***Filiform papillae*:** After development of the primordium at E17 (Fig. 3j) on filiform papillae, the connective tissue core of filiform papillae was clearly observed with a rapid thickening of epithelial tissues from E18 to E19 (Fig. 7a). VEGF was expressed in the cytoplasm of growing epithelial cells at E19, but capillary sprouts invaded into connective tissue cores were not observed (Figs. 7b, c). At E20, a keratinized layer uniformly stained with eosin was observed on the surface layer of epithelial tissues. Although differentiation specific to epithelial tissues of filiform papillae was not observed yet, a cell layer with keratohyalin granules was observed under the keratinized layer, and mitotic epithelial cells were observed only in the basal layer (Fig. 7d). Invasion by blind-ended capillary sprouts was observed from the subepithelial sinusoidal capillaries into the connective tissue core of filiform papillae (Fig. 7e). At P1, epithelial differentiation to the three types of epithelia (anterior papillae, posterior papillae, and interpapillary epithelium) was observed in epithelial tissues of filiform papillae, and the basic morphology of filiform papillae was completed (Fig. 7f). With epithelial differentiation of filiform papillae, capillary sprouts of the connective tissue core became loop shaped (Fig. 7g). At P7, epithelial tissues had further matured and thickened, and the interpapillary epithelium between filiform papillae was expanded. With maturation of muscle and fat tissues, blood vessels running between connective tissues became denser, and the vascular lumen was more expanded (Figs. 7h, i).

Morphogenesis of the rat tongue, development of each lingual papillae, expression of VEGF and angiogenesis in lingual papillae are summarized to Fig. 8.

DISCUSSION

This is the first paper reporting angiogenesis and expression of VEGF during morphogenesis of lingual papillae in rats. As previously reported, with respect to morphology of each papilla in adult rat, circumvallate

papillae and foliate papillae contain taste buds in the lateral papillary epithelium, and serous glands are observed at the bottom of furrows. Fungiform papillae are dome shaped eminences having one taste bud in the dorsum of the tongue [7,28,29]. It was reported that there were 3 types of filiform papillae in adult rat depending on the region of the dorsum of the tongue, and epithelial tissues showed 3 types of differentiation and keratinized layers having different characteristics [1,5,8]. The same morphology of papillae in the adult rat reported by previous authors was observed in our study.

Morphogenesis of the rat tongue and lingual papillae

Morphogenesis of the rat tongue and lingual papillae are summarized to Fig. 8. The primordium of the rat tongue develops at E13 by fusion of lateral lingual swellings and hypobranchial eminence [28,29]. In our study, we observed the lingual primordium at E13, the mandible and tongue were clearly distinguished at E14, and basic morphology of the tongue was confirmed. Theories on development of lingual papillae slightly differ depending on observers, but it is accepted that the primordium of circumvallate papillae is the first stage in lingual development, followed by developments of the primordium of fungiform papillae, foliate papillae, and filiform papillae, respectively [4,5,30,31]. The primordium of circumvallate papillae was also initially observed in our study at E13 together with development of the lingual primordium, followed by developments of the primordium of fungiform papillae, foliate papillae, and filiform papillae at E14, E16, and E17, respectively. Development of lingual papillae was observed as local changes in epithelial tissues on the basement membrane. In other words, primordia of circumvallate papillae and foliate papillae were confirmed by local proliferation of epithelial tissues, whereas the primordia of fungiform papillae and filiform papillae were confirmed by meandering of epithelial tissues on the basement membrane. Considering that Sonic hedgehog is closely involved in morphogenesis of lingual papillae, and from data of lingual developments from E14 to E16 of the epithelial basement membrane and the connective tissue core just under the epithelium of fungiform papillae [9], we hypothesize that there may be a close relationship between epithelial tissues and the connective tissue with respect to morphogenesis of lingual papillae.

At E19, morphology of the lingual papillae was similar to that in adult rat with a thickened epithelium, and it was reported that the basic shape of lingual papillae was observed from E20 to P1 [4,5,8,32]. The keratinized layer of each papilla was also observed at E20 in our study, and development of taste buds was confirmed on circumvallate papillae, fungiform papillae, and foliate papillae at P1. At this stage, differentiations of the 3 specific epithelial tissues were observed in filiform papillae, and basic morphology of each papilla was confirmed. Observations in this study suggested that specific morphology of each papilla accompanied by development of a taste bud takes place relatively late from E20 to P1. Timing of development of human taste buds greatly varies from fetal day 8 to week 28 depending on different studies, due to difficulties in collecting samples [33,34], but differences with the rat lie in the fact that human taste buds develop relatively early during the fetal period.

Tissue differentiation and angiogenesis of the tongue epithelium

Expression of VEGF and angiogenesis in lingual papillae are summarized to Fig. 8. Dense sinusoidal capillaries develop subepithelially on the dorsum of the tongue from the lingual artery that runs deep in the lingual muscle in the tongue of adult rat, and a loop shaped vascular network extends from sinusoidal capillaries to the lingual papillae to feed lingual papillary epithelial tissues [2,3,10,35]. It is known that blood vessels develop by either vasculogenesis or angiogenesis. In vasculogenesis, the primary capillary plexus is considered to develop from a blood island, inducing hemangioblasts in the mesoderm [12,15]. On the contrary, angiogenesis involves sprouting and intussusception, and blood vessels develop by repeating fusion, branching, and pruning in response to organ morphogenesis (vascular remodeling). The mature vascular system is completed when differentiation of mural cells is observed (vascular myogenesis) [13,14,20]. With regards to the embryonic vascular system in rat, endothelial cells form the lumen of the dorsal aorta which develops at an earliest stage at E12, and mesenchymal cells differentiate to mural cells from E13 to E16 [36]. For angiogenesis of lingual papillae, it is reported that blind-ended neovascularity occurs at E20 in filiform papillae, at which time epithelial tissues are specifically differentiated, and a loop shaped vascular network is observed at P1 [11].

In this study, aggregates of cells suggested to correspond to the blood island were observed subepithelially on the tongue primordium at E13. These aggregates consisted of peripheral cells, suggestive of oval angioblasts and hemopoietic cells in the center of the aggregates, as seen in a blood island. Subepithelial endothelial cells became flat throughout development of

muscle tissues at E15, blood cells in the vascular lumen became denucleated at E16 when fusion and branching of vascular lumens had progressed, and dense subepithelial sinusoidal capillaries were observed at E17. It is considered that subepithelial sinusoidal capillaries of the dorsum of the tongue developed by vasculogenesis because aggregates similar to a blood island. Blood vessels between muscle tissues formed a layer of endothelial cells by E18, and active proliferation of endothelial cells was observed whereas numerous differentiated mural cells were observed around endothelial cells from E19 onwards, when the epithelium became extremely thick. We concluded that angiogenesis by vascular remodeling actively took place in blood vessels between muscle tissues by E18, and the vascular lumen was enlarged by vascular myogenesis from E19 onward.

Angiogenesis was not observed in lingual papillae at early stages of development, and this may be because oxygen and nutritional requirements of tissues were fully satisfied by diffusion from subepithelial sinusoidal capillaries when the epithelial tissue was undifferentiated and expansion of the connective tissue core was slow. However, in circumvallate papillae, fungiform papillae, and filiform papillae in which thickening of epithelial tissues and expansion of the connective tissue core became prominent, VEGF was expressed around the fibroblasts of the expanded connective tissue core and basement membranes of epithelial tissues, and angiogenesis was confirmed on the following days. Blind-ended neovascularity of sprouting was observed especially in fungiform papillae and filiform papillae. It is considered that acceleration of angiogenesis by VEGF is associated with increased requirements of oxygen and nutrients by morphogenesis of lingual papillae. In foliate papillae which develop by epithelial depression, VEGF was observed in small amounts around basement membranes of epithelial tissues, and angiogenesis of intussusception was observed where the existing thin, linear blood vessels became dense in a plexus state by proliferation. Our observations showed that VEGF was locally expressed in lingual papillae prior to angiogenesis, suggesting a close involvement of VEGF in angiogenesis of lingual papillae. When timings of angiogenesis of blood vessels and vascular network were compared between the 4 types of lingual papillae, absolute amount of the connective tissue core was minimal in filiform papillae lacking taste buds, and angiogenesis into the connective tissue papillae was also delayed. Therefore, oxygen and nutritional requirements are considered to be relatively lower to other lingual papillae containing taste buds. The loop shaped vascular network is established in each subepithelial papilla by birth, and timing is very close to differentiation of the primordium of taste buds and epithelial tissues of filiform papillae, suggesting a close relationship between higher differentiation of epithelial tissues and development of the vascular system.

Differentiation of taste buds was reported by several researchers, and a close relationship between development of taste buds and that of the nervous system has been demonstrated [37,38]. During early developmental stages, invasion of nerve fibers into circumvallate papillae and fungiform papillae was particularly reported at E16 [29,30,32]. Although an integrated report on vascular and nervous systems related to morphogenesis of lingual papillae has not been published yet, our study suggested that subpapillary invasion took place at an earlier age in the nervous system compared to the vascular system.

We reported that VEGF expression was closely involved in morphogenesis of lingual papillae and angiogenesis of lingual papillae, and a close relationship existed between higher differentiation of lingual papillary epithelial tissues and development of the respective vascular system.

ACKNOWLEDGMENTS: We would like to thank the late professor Mitsuaki Yoshizuka, our mentor, for his kind and unlimited guidance.

REFERENCES

1. Kutuzov H, and Sicher H. The filiform and the conical papillae of the tongue in the white rat. Anat Rec 1951; 110:275-288.
2. Nagato T, Nagaki M, Murakami M, and Tanioka H. Morphological studies of rat lingual filiform papillae. Okajimas Folia Anat Jpn 1989; 66:195-210.
3. Ojima K, Ogura K, Sato T, and Niwa M. Microvascular cast specimen formation of lingual papillae in zinc-deficient rat tongue. Ann Anat 1999; 181:371-375.
4. Kiyonaga M. An embryologic study on the tongue's papillae and taste buds in the rat. J Kyusyu Dent Coll 1957; 11:117-139. (in Japanese)
5. Farbman AI. The dual pattern of keratinization in filiform papillae on rat tongue. J Anat 1970; 106:233-242.
6. Mistretta CM. Topographical and histological study of the developing rat tongue, palate and taste buds. In: Third Symposium on Oral Sensation and Perception: The Mouth of the Infant, ed. Bosma JF, Springfield, Thomas, pp 163-187, 1972.
7. Mistretta CM, and Baum BJ. Quantitative study of taste buds in fungiform and circumvallate papillae of young and aged rats. J Anat 1984; 138:323-332.
8. Iwasaki S, Aoyagi H, and Yoshizawa H. Immunohistochemical detection of the expression of kera-

tins 14 in the lingual epithelium of rats during the morphogenesis of filiform papillae. Arch Oral Biol 2003; 48:605-613.
9. Mistretta CM, Liu HX, Gaffield W, and MacCallum DK. Cyclopamine and jervine in embryonic rat tongue cultures demonstrate a role for Shh signaling in taste papilla development and patterning: fungiform papillae double in number and form in novel location in dorsal lingual epithelium. Dev Biol 2003; 254:1-18.
10. Makiyama MCK, Watanabe IS, Mizusaki CI, and Junior BK. Three-dimensional angioarchitecture of tongue corrosion casts from normal young rats. Ann Anat 1998; 180:327-330.
11. Okada S, and Aharinejad S. Lingual papillae of the growing rat as a model of vasculogenesis. Anat Rec 1997; 247:253-260.
12. Risau W, and Flamme I. Vasculogenesis. Annu Rev Cell Dev Biol 1995; 11:73-91.
13. Risau W. Mechanisms of angiogenesis. Nature 1997; 386:671-674.
14. Takakura N, Watanabe T, Suenobu S, Yamada Y, Noda T et al. A role for hematopoietic stem cells in promoting angiogenesis. Cell 2000; 102:199-209.
15. Parker LH, Schmidt M, Jin SW, Gray AM, Beis D et al. The endothelial-cell-derived secreted factor Egfl7 regulates vascular tube formation. Nature 2004; 428:754-758.
16. Senger DR, Galli SJ, Dvorak AM, Perruzzi CA, Harvey VS et al. Tumor cells secrete a vascular permeability factor that promotes accumulation of ascites fluid. Science 1983; 219:983-985.
17. Ferrara N, and Henzel WJ. Pituitary follicular cells secrete a novel heparin-binding growth factor specific for vascular endothelial cells. Biochem Biophys Res Commun 1989; 161:851-858.
18. Folkman J, and Klagsbrun M. Angiogenic factors. Science 1987; 235:442-447.
19. Neufeld G, Cohen T, Gitay-Goren H, Poltorak Z, Tessler S et al. Similarities and differences between the vascular endothelial growth factor (VEGF) splice variants. Cancer Metastasis Rev 1996; 15:153-158.
20. Beck JRL, and D'Amore PA. Vascular development: cellular and molecular regulation. FASEB J 1997; 11:365-373.
21. Ferrara N, and Davis-Smyth T. The biology of vascular endothelial growth factor. Endocr Rev 1997; 18:4-25.
22. Fava RA, Olsen NJ, Spencer-Green G, Yeo KT, Yeo TK et al. Vascular permeability factor/Endothelial Growth Factor (VPF/VEGF): accumulation and expression in human synovial fluids and rheumatoid synovial tissue. J Exp Med 1994; 180:341-346.
23. Ichigatani M, Saga T, Yamaki K, and Yoshizuka M. Appearance of vascular endothelial growth factor (VEGF) in femoral head in the growing rat. Histol Histopathol 2001; 16:463-468.
24. Maejima M, Maruoka Y, Sawada T, Ando T, Kobayashi M et al. Expression of vascular Endothelial Growth Factor (VEGF) and specific receptors (Flt-1 and Flk-1) in rat tongue Carcinogenesis Induced by 4-Nitroquinoline 1-Oxide. Acta Histochem Cytochem 2002; 35:331-341.
25. Poltorak Z, Cohen T, Sivan R, Kandelis Y, Spira G et al. $VEGF_{145}$, a secreted vascular endothelial growth factor isoform that binds to extracellular matrix. J Biol Chem 1997; 272: 7151-7158.
26. Tischer E, Mitchell R, Hartman T, Silva M, Gospodarowicz D et al. The human gene for vascular endothelial growth factor. Multiple protein forms are encoded through alternative exon splicing. J Biol Chem 1991; 266: 11947-11954.
27. Okawa K. The fine structure of the coagulating gland in the mouse. J Kurume Medical Association 1986; 49:81-95. (in Japanese)
28. Shimizu Y. Generation and development of neural elements distributed in the rat's tongue. J Kyusyu Dent Coll 1987; 41:345-360. (in Japanese)
29. Ohmura Y. Studies on morphogenesis and histodifferentiation of the rat tongue. J Fukuoka Dent Coll 1999; 26:159-178. (in Japanese)
30. Farbman AI, and Mbiene JP. Early development and innervation of taste bud-bearing papillae on the rat tongue. J Comp Neurol 1991; 304:172-186.
31. Mbiene JP, and Mistretta CM. Initial innervation of embryonic rat tongue and developing taste papillae: nerves follow distinctive and spatially restricted pathways. Acta Anat 1997; 160:139-158.
32. Hirata K, and Kanaseki T. Immunohistochemical studies on neuron-specific enolase in developing rat vallate papillae. Anat Embryol 1989; 180:159-163.
33. Bradley RM, and Stern IB. The development of the human taste bud during the foetal period. J Anat 1967; 101:743-752.
34. Vij S, and Kanagasuntheram R. Development of the nerve supply to the human tongue. Acta Anat 1972; 81:466-477.
35. Shimizu T. The lingual artery of the rat. Okajimas Folia Anat Jpn 1986; 63:47-66.
36. Nakamura H. Electron microscopic study of the prenatal development of the thoracic aorta in the rat. Am J Anat 1988; 181:406-418.
37. Mistretta CM, Goosens KA, Farinas I, and Reichardt LF. Alterations in size, number and morphology of gustatory papillae and taste buds in BDNF null mutant mice demonstrate neural dependence of developing taste organs. J Comp Neurol 1999; 409:13-24.
38. Sollars SI. Chorda tympani nerve transection at different developmental ages produces differential effects on taste bud volume and papillae morphology in the rat. J Neurobiol 2005; 64:310-320.

Original Contribution

Kurume Medical Journal, 54, 25-29, 2007

GnRH Agonist Acts as Ovarian Protection in Chemotherapy Induced Gonadotoxicity: An Experiment Using a Rat Model

GO MATSUO, KIMIO USHIJIMA, ATSUHIKO SHINAGAWA*, SYUN-ICHI TAKAHASHI, NAOKI FUJIYOSHI, SYUJI TAKEMOTO, ATSUMU TERADA, AKIMASA FUKUI AND TOSHIHARU KAMURA

*Department of Obstetrics and Gynecology, Kurume University School of Medicine, Kurume 830-0011 and *Shinagawa Hospital, Iki 811-5132, Japan*

Received 18 December 2006, accepted 3 August 2007

Edited by KENTARO YAMADA

Summary: To reduce chemotherapy induced gonadotoxicity, co-treatment with gonadotropin releasing hormone against analogue (GnRHa) was tested using rat model. Leuprorelin acetate (Leuplin) with or without cisplatin (CDDP) was given subcutaneously at a dose of 9.4 μg/ml to Wistar strain female rats. The total number of follicles was counted and the maturation of follicles was evaluated at the largest section of the ovary on the 5th and 10th day after administration. Leuplin led the ovary to a resting phase in which primordial follicle occupied 80% of all follicles in only 5 days after administration. The serum E2 level was also down by the 5th day and maintained a low level to the 10th day. In co-treatment with GnRHa and CDDP rats, the primordial follicle occupied 90% of all follicles and the total number of follicles was higher than in CDDP alone rats. This rat model verified that GnRHa co-treatment well minimized CDDP induced gonadotoxocity by desensitization of the ovary. These results were promising for the clinical application introducing GnRHa co-treatment as ovarian protection in cancer chemotherapy in young women.

Key words GnRH agonist, chemotherapy related amenorrhea, ovarian protection, apoptosis

INTRODUCTION

Recent advances in cancer chemotherapy have helped cancer survivors achieve long disease free interval. Young male and female patients with germ cell tumor, genital cancer, hematologic malignancies, or pediatric malignancies suffer from sexual dysfunction resulting in infertility. Chemotherapy induced ovarian toxicity by cyclophosphamide was introduced to breast cancer patients in the late 70's [1]. Unlikely the situation in other organs, heavy ovarian toxicity is irreversible, because the number of follicles is limited. Whereas dose intensive chemotherapy including hematopoietic or stemcell transplantation has been widely accepted for young patients, the risk of chemotherapy-related amenorrhea (CRA) has increased with the age at the time of treatment, in a dose-dependent manner [2]. Even in adolescence, survivors had a risk of menopause four times greater than that of control healthy girls between the ages of 21 and 25 [3]. Nevertheless, ovarian function was often preserved in survivors who were treated prepubertally [3,4]. Gonadotropin releasing hormone agonist analogue (GnRHa) is widely used for endometriosis, and is also available for estrogen dependent tumors, such as leiomyoma, and breast cancer, as medical castration. The aim of GnRHa application in young patients is to inactivate their ovarian function temporarily, and may protect them from CRA. In this report, we tested co-treatment GnRHa with cisplatin (CDDP) using the rat model and inves-

Corresponding author: Kimio Ushijima, Department of Obstetrics and Gynecology, Kurume University School of Medicine, 67 Asahi-machi, Kurume 830-0011, Japan. Tel: +81-942-31-7573 Fax: +81-942-35-0238 E-mail: kimi@med.kurume-u.ac.jp

Abbreviations: CDDP, cisplatin; CRA, chemotherapy related amenorrehea; GnRHa, gonadotropin releasing hormone agonist analogue; RIA, radioimmunoassay.

tigated whether or not it would reduce chemotherapy-induced gonadotoxicity.

MATERIALS AND METHODS

Animals

Five-week old matured female Wistar strain rats were used for this experiment.

Chemicals

Leuprorelin Acetate (Leuprin, Takeda Pharmacia Company, Tokyo, Japan) was prepared with an attached suspension at a concentration of 9.4 μg/ml, corresponding to the 50 μg/kg conventional dose for humans. CDDP (Randa, Nippon Kayaku ltd., Tokyo, Japan) solution (0.5 mg/ml) was prepared at a concentration of 10.1 mg/kg corresponding to 1/2 LD50 of the rat, which was divided over 5 days of administration. Each solution was diluted to 2 ml with 0.9% saline.

Treatment schedule

Experiment 1: To evaluate the gonadal effect of leuprin on untreated rat ovary: Leuprin was injected subcutaneously to 28 rats. Eighteen rats were sacrificed at day 5 (1 menstrual cycle: GnRHa 1 cycle rats) and 10 rats were sacrificed at day 10 (2 menstrual cycles: GnRHa 2 cycle rats). Bilateral ovaries were removed under ether anesthesia on sacrifice. Eight untreated rats were prepared as control, and were sacrificed on the same days and their ovaries also removed.

Experiment 2: To examine the effect of co-treatment of CDDP and GnRHa: Leuprin was injected into 13 rats, in the same way as in experiment 1. CDDP was administered intraperitoneally for 5 days, 5 days after leuprin injection (CDDP+GnRHa rats). The total dose of CDDP was 10.1 mg/kg. The rats were sacrificed 24 hrs after the final CDDP administration. CDDP solution alone was injected into 19 rats for 5 days and they were then sacrificed to remove their ovaries (CDDP rats). Bilateral ovaries were removed in both groups. Only normal saline was injected into 8 rats in the control group, on the same schedule as CDDP rats.

The body weights of the rats were examined at the beginning and the end of the experiment for all groups.

Histological examination

Excised ovaries were fixed in formalin and paraffin embedded and stained with hematoxylin and eosin. They were sectioned into 4 μm sliced continuous sections. The number of follicles was counted by a light microscope at maximum diameter. The maturation of follicles was estimated by modified Pederson and Peters classification (Table 1) [5]. Precisely, follicles were classified into 8 subgroups by the number of layers of granulose cells and the maximum diameter of follicles. Furthermore, the total number of follicles in each group was calculated, and once again divided into 3 groups, small (immature), medium, and large (matured) follicle groups.

TABLE 1.
Classification of follicles for maturation evaluation

Classification	Subtype	Number of layer*	Diameter (μm)**
Small	type 1	none	～6
	type 2	incomplete	～10
	type 3a	single	～15
Medium	type 3b	single	～30
	type 4	two	～50
	type 5a	three	～60
Large	type 5b	four	～80
	type 6	five	～120
	type 7	cumulus	～200
	type 8	well formed cumulus	～350

* Number of layers of granulosa cells
** Maximum diameter of follicles

Biochemical Analysis

Serum levels of estradiol (E2) were examined by RIA using the rat E2 ^{125}I kit (Amersham) in experiment 1.

Statistics

Data was presented as mean±SD. Statistical significant was analysis by the Mann &Whitney test for the comparison of the number of follicles in each group. A value of $P<0.05$ was considered significant.

RESULTS

Experiment 1

The total number of follicles was counted and the mean number of follicles was compared among the three groups. Significant loss of follicles was found in GnRHa 1 cycle and 2 cycle rats. There was a statistical

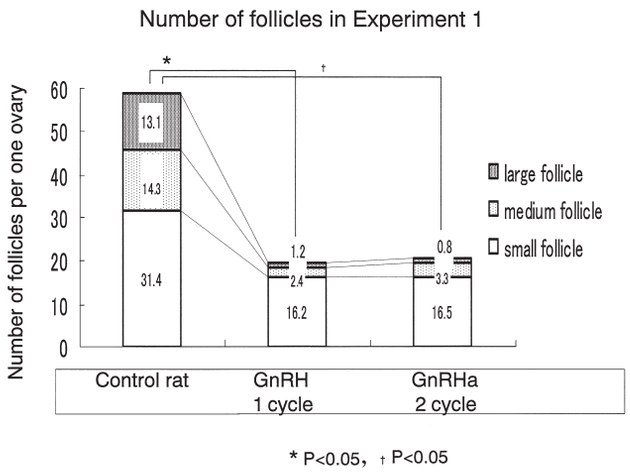


Fig. 1. Total number of follicles significantly decreased in GnRHa rats. Medium and large follicles were lost in GnRHa rats. No difference was found between GnRHa 1 cycle and 2 cycle treatment.

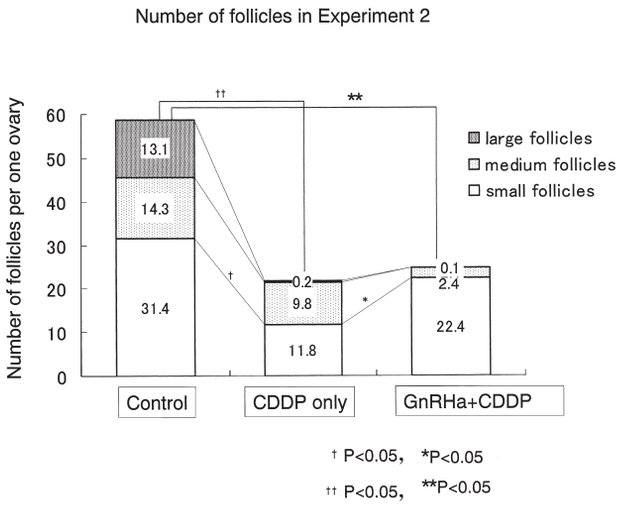


Fig. 3. The number of total follicles significantly decreased in CDDP rats and GnRHa+CDDP rats. A larger number of small follicles were preserved in GnRHa+CDDP rats than CDDP rats.

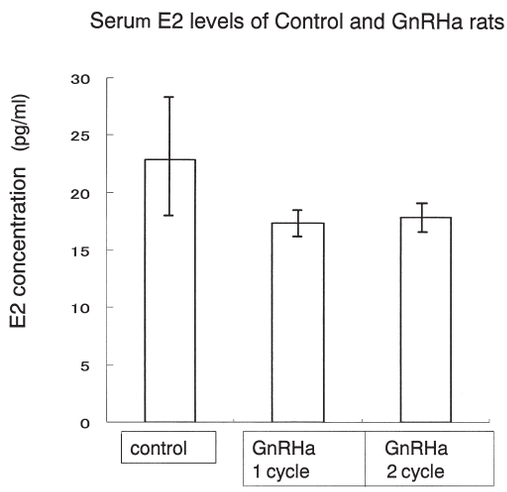


Fig. 2. GnRHa rats showed lower tendency of serum E2 levels than control rats. No difference was found between GnRHa 1 cycle and 2 cycle treatment.

difference in the loss of follicles between the control rats and GnRHa 1 cycle and 2 cycle rats ($P<0.05$). The mean numbers of follicles in each group were 58.8, 19.8, and 20.6 per ovary, in the control, GnRHa 1 cycle and 2 cycle rats, respectively. Also, there was a difference in the distribution of follicle subtypes between the control and GnRHa rats. Medium and large follicles were significantly lost in GnRHa rats. As a result, the rate of small follicles in GnRHa rats was higher than that in control rats. The rate of small follicles among the total number of follicles in control rats, GnRHa 1 cycle rats and GnRHa 2 cycle rats were 54.4%, 80.0% and 80.1%, respectively. There was no difference in the total number of follicles and the rate of small follicles between GnRHa 1 cycle and 2 cycle rats (Fig. 1). The serum levels of E2 in GnRHa 1 cycle and 2 cycle rats showed a similar tendency (not significant) of decline from that in the control rats (Fig. 2).

Experiment 2

A significant loss of follicles was found in GnRHa+CDDP rats and CDDP rats comparing to control rats. Although, there was no difference in the total number of follicles between GnRHa+CDDP rats and CDDP rats, a larger number of small follicles were preserved in GnRHa+CDDP rats than CDDP rats (GnRHa+CDDP rats : 22.4±6.3 vs. CDDP rats: 11.8±6.3). The rate of small follicles among the total follicles in CDDP rats and GnRHa+CDDP rats were 54.1% (11.8/21.8) and 90.0% (22.4/24.9) respectively (Fig. 3). There were no rats having body weight loss exceeding 20% of their original weight.

DISCUSSION

Chemotherapy-induced gonadotoxicity is a state of hypergonadotropic hypogonadism. It caused CRA and finally irreversible ovarian failure in women. Histologically, focal or diffuse cortical fibrosis, reduction in follicle numbers, and impaired follicular maturation were observed in the ovary obtained from autopsy

cases, and those findings were independent of pubertal age [6]. The risk of gonadal damage is directly related to the age of the patient. Chapman et al. [7] reported a higher incidence of ovarian failure in patients older than 30 years of age after completion of chemotherapy in Hodgkin lymphoma. In breast cancer, no patients under 30 years of age showed CRA for doxorubicin-containing regimen, 33% of patients between 30 and 39 years showed CRA, and 96% of patients between 40 and 49 years showed CRA [8]. Shinagawa [9] demonstrated antral (large) follicle was more sensitive to cytotoxic chemotherapeutic agent than primordial (small) follicle in rat models. In prepubertal girls, less than 10% had ovarian dysfunction due to alkylating agents [10]. The large number of primordial follicles in the prepubertal ovary may contribute to resistance to cytotoxic chemotherapy [11]. Ataya et al. [12] tested co-treatment of cyclophosphamide and GnRHa in rat models. GnRHa inhibited follicle maturation from primordial follicles to antral follicles. As a result, primordial follicle dominant ovary was well protected from cyclophophamide-induced gonadotoxicity. Co-treatment of GnRHa with anticancer agent seems to be favorable as ovarian protection from gonadotoxicity in cancer chemotherapy.

In clinical application of ovarian protection by GnRHa, Waxman et al. [13] failed to verify the effectiveness of co-treatment of buserelin with anticancer drugs in the treatment of Hodgkin lymphoma. Blumenfeld et al. [14], however, reported a higher incidence of lymphoma patients who resumed spontaneous ovulation among patients treated with GnRHa and anticancer agents than patients with chemotherapy alone (96% versus 35%). There are several conceivable reasons for this discrepancy. In our experiments, only a 5-day interval from GnRHa administration was enough to introduce the resting phase to the rat ovary in which primordial follicles were dominant. It demonstrated that pituitary-ovarian desensitization by GnRHa administration was completed quickly in the rat, because the rat menstrual cycle is very short. This was also verified by a prompt decline in serum E2 level. Nevertheless, significance of decreasing of E2 was not shown in this experiment. Small amount of preserved medium follicle in GnRHa rats could become a source of E2 production.

Direct suppression of GnRH receptors in rat ovary was helpful in this rapid completion of desensitization [15]. Meanwhile, human ovary has a much lower concentration of GnRH receptor than rat ovary [14]. It is supposed to take a longer interval to desensitize human ovary. Waxman's study failed to protect ovarian function, because patients in that study did not have enough time for desensitization before initiating chemotherapy. For a better result of ovarian protection, GnRHa administration should be started as soon as possible to protect antral follicles during the first course of chemotherapy.

GnRHa induced apoptosis in rat granulosa cells [16]. By this GnRHa direct effect on the ovary, loss of follicles was observed in GnRHa treated rats in our experiment. Nevertheless, in the human ovary, apoptosis by GnRHa will not be a serious problem. It should appear less frequently because of lower concentrations of GnRH receptor in human ovary.

Among many anticancer agents, cyclophosphamide was the most frequently tested drug for gonadal toxicity in animal models. Although CDDP is one of the most available drugs in gynecologic cancer, there have been few reports on gonadal toxicity. Wallace et al. [17] reported that a higher dose of CDDP revealed higher rates of gonadotoxicity in chemotherapy for human osterosacoma. Maneschi et al. [18] reported only 2 cycles of relatively high dose CDDP plus bleomycin induced CRA in advanced cervical cancer. So CDDP induced gonadotoxicity is worthy of discussion. Shinagawa [9] reported CDDP induced ovarian toxicity occurred in a dose and time dependent manner in rat models, and we demonstrated co-treatment with GnRHa worked well as ovarian protection.

Chemotherapy related ovarian failure may cause the patient to loose quality of life, with vasomotor symptoms, vaginal dryness, body weight gain, rapid bone loss and risk of subsequent fracture [19]. The effectiveness of goserelin (zoradex) as medical castration was indicated in chemotherapy for premenopausal breast cancer patients. Goserelin and cyclophophumide, methotrexate, and fluorouracil (CMF) chemotherapy showed similar survival to the patients treated by CMF alone. Co-treatment of goserelin showed not only an additive effect of chemotherapy but also that it worked as ovarian protection. Ovarian function was reversible in patients under 40 years of age [20]. As the number of younger patients who receive chemotherapy increases, clinical application of ovarian protection becomes more and more interesting. Based on our experiments, the protective effects of GnRHa against CDDP induced gonadotoxicity were verified in rat model. These results encourage us to introduce some clinical trials as a pilot study. In order to obtain a long time follow up of ovarian function, collaboration with other institutions should be initiated.

ACKNOWLEDGMENTS: The authors thank Dr. Takashi

Nishida for instruction for research and Ms Yaeko Namatsu for the technical assistance of animal experiments.

REFERENCES

1. Koyama H, Wada T, Nishizawa Y, Iwanaga T, Aoki Y et al. Cyclophosphamide-induced ovarian failure and its therapeutic significance in patients with breast cancer. Cancer 1977; 39:1403-1409.
2. Horning SJ, Hoppe RT, Kaplan HS, and Rosenberg SA. Female reproductive potential after treatment for Hodgkin's disease. N Eng J Med 1981; 304:1377-1382.
3. Byrne J, Fears TR, Gail H, Pee D, Connelly RR et al. Early menopause in long-term survivors of cancer during adolescence. Am J Obstet Gynecol 1992; 166:788-793.
4. Ortin TT, Shoshlak CA, and Donaldson SS. Gonadal status and reproductive function following treatment for Hodgkin's disease in childhood: the Stanford experience. Int J Radiol Oncol Biol Phys 1990; 19:873-880.
5. Pedersen T, and Peters H. Proposal for a classification of oocyte and follicles in the mouse ovary. J Reprod Fertile 1968; 17:555-557.
6. Nicosia SV, Matus-Ridley M, and Meadows AT. Gonadal effects of cancer therapy in girls. Cancer 1985; 55:2346-2372.
7. Chapman RM, Sutcliffe SB, and Malpas JS. Cytotoxic-induced ovarian failure in women in Hodgkin's disease. JAMA 1979; 242:1877-1881.
8. Hortobagyi GN, Buzdar AU, Marcus CE, and Smith TL. Immediate and long-term toxicity of adjuvant chemotherapy regimens containing doxorubicin in trials at M. D. Anderson Hospital and Tumor Institute. NCI Monogr 1986; 1:105-109.
9. Shinagawa A. Cisplatin induced ovarian toxicity in rats-An experimental analysis-. J Kurume Med Assoc 1998; 61:220-226. (in Japanese)
10. Siris ES, Leventhal BG, and Vaitukaitis JL. Effects of childhood leukemia and chemotherapy of puberty and reproductive function in girls. N Engl J Med 1976; 294:1143-1146.
11. Damewood MD, and Grochow LB. Prospecis for fertility after chemotherapy or radiation for neoplastic disease. Fertile Sterile 1986; 45:443-450.
12. Ataya KM, McKenna JA, Weintraub AM, Clark MR, and Lemaire WJ. A Latinizing Hormone-releasing hormone agonist for the prevention of chemotherapy-induced ovarian follicular loss in rats. Cancer Research 1985; 45:3651-3656.
13. Waxman JH, Ahmed R, Smith D, Wrigley PF, Gregory W et al. Failure to preserve fertility in patients with Hodgkin's disease. Cancer Chemother Pharmacol 1987; 19:159-162.
14. Blumenfeld Z, Avivi I, Linn S, Epelbaum R, Ben-Shahar M et al. Prevention of irreversible chemotherapy-induced ovarian damage in young women with lymphoma by a gonodotropin-releasing hormone agonist in parallel to chemotherapy. Human Reprod 1996; 11:1620-1626.
15. Ataya K, and Moghissi K. Chemotherapy-induced premature ovarian failure: Machanisms and prevention. Steroids 1989; 54:607-626.
16. Billig MC, Furuta I, and Hsueh AJ. Gonadotropin-Releasing Hormone Directly Induces Apoptotic Cell Death in the Rat Ovary: Biochemical in Situ Detection of Deoxyribonucleic Acid Fragmentation in granulose cells. Endocrinology 1994; 134:245-252.
17. Wallace WHB, Shalet SM, Crowne EC, Morris-Jones PH, Gattamaneni HR et al. Gonadal dysfunction due to Cisplatin. Medical and Pediatric Oncology 1989; 17:409-413.
18. Maneschi F, Benedetti-Panichi G, Scambia G, Salerno G, Agostino D et al. Menstrual and Hormone Patterns in Women Treated with High-Dose Cisplatin and Bleomycin. Gynecol Oncol 1994; 54:345-348.
19. Shapiro CL, Manola J, and Leboff M. Ovarian failure after adjuvant chemotherapy is associated with rapid bone loss in women with early-stage breast cancer. J Clin Oncol 2001; 19:3306-3311.
20. Recchika F, Saggio G, Amiconi G, Blasio AD, Candeloro G et al. Gonadotropin-releasing hormone analogues added to adjuvant chemotherapy protect ovarian function and improve clinical outcomes in young women with early breast carcinoma. Cancer 2006; 106:514-523.

Original Contribution

Kurume Medical Journal, 54, 31-34, 2007

Simple Limbectomy Dose not Affect the Growth of the Acetabulum: An Experimental Study

TAKETOSHI KANAZAWA, TAKAHIKO SANNOMIYA, TAKAHIRO OKAWA, MASAFUMI GOTOH*, FUJIO HIGUCHI*, AKIO INOUE** AND KENSEI NAGATA

Department of Orthopaedic Surgery, Kurume University School of Medicine, Kurume 830-0011
**Deptrtment of Orthopaedic Surgery, Kurume University Medical Center, Kurume 830-0863 and **Yanagawa Rehabilitation Hospital, Yanagawa 832-0058, Japan*

Received 13 November 2006, accepted 29 October 2007

Edited by NAOTO SHIBA

Summary: Little is known about the influence of simple limbectomy on the growth of the acetabulum. An experimental study was carried out in ten monkeys divided into two groups: limbectomy only (Group A) and limbectomy with concomitant cartilage resection (Group B). After three years and four months postoperatively, monkeys were sacrificed. Excised joints were examined macro-and microscopically. Degenerative changes in the cartilage and hypertrophy in the joint capsule were noted in all five monkeys of Group B, and in none of Group A. The diameter of the acetabulum was significantly enlarged in Group B (longitudinal diameter: $p<0.05$, transverse diameter: $p<0.01$, Mann-Whitney's U test), compared with Group A and the contralateral hips as controls. There was no other significant difference in other soft tissue or osseous components, between two groups. Histologically, the injured limbus was healed with irregular and sparse fibrous tissue in both groups. Fibrillation in the superficial layer of the cartilage and cluster formation was frequently noted in group B, while normal appearance was noted in Group A. This study demonstrated that simple limbectomy dose not affect the growth of the acetabulum, but may cause degenerative changes if the adjacent acetabular cartilage was simultaneously injured.

Key words limbectomy, hip joint, acetabulum growth, cartilage injury

INTRODUCTION

The limbus in the hip joint is a fibrous tissue surrounding the acetabular margin, which contributes to the stability of the femoral head in the joint [1-3]. Interposition of the limbus is clinically known to be one of difficult reduction and retention in congenital dislocation of the hip. Surgical excision of the interposed limbus has, however, been controversial, since there are certain problems that can lead to secondary osteoarthritis of the joint [4,5].

Concerning this, there could be technical problems at the time of surgery related to any concomitant cartilage injury. We therefore hypothesized that simple limbectomy does not affect the growth of the acetabulum, but when the acetabulum is accompanied by concomitant cartilage injury then growth might be affected. An animal experiment using monkey that has hip limbus similar to that in human [6] was undertaken to investigate this hypothesis.

MATERIALS AND METHODS

Ten one-year-old Japanese monkeys (Macaca fuscata) with an average body weight of 1056 g (820-1430 g) were bred at Kurume University Animal

Correspondence: Taketoshi Kanazawa, M.D., Department of Orthopaedic Surgery, Yanagawa Rehabilitation Hospital, 113-2 Kamimiyanaga-machi, Yanagawa 832-0058, Japan. Tel: 0944-72-0001 Fax: 0944-72-1127

Center from 1996 to 2001, and were used in this study.

The monkeys were anesthetized intramuscularly with ketamine hydrochloride (20 mg/kg body weight). Limbectomy was performed at the dorsal limbus of the load-bearing portion through a posterior approach (Fig. 1). According to the presence or absence of injury to the acetabular cartilage, the monkeys were divided into two groups: Group A with simple limbectomy, and Group B with limbectomy and cartilage injury. In Group B, the acetabular cartilage was resected as shown in Fig. 2. At this time, great care was taken not to damage the femoral head in both groups. The contralateral hip joints were untreated as control.

After three years and four months postoperatively, the monkeys were sacrificed under deep anesthesia (general anesthesia), confirming cardio-pulmonary arrest and pupils dilated. After extirpation the bilateral hip joints, the joints were macroscopically observed for hypertrophy in the limbus, degenerative change in the cartilage (acetabulum and femoral head), the diameter of the acetabulum (longitudinal and transverse), any deformity in the femoral head, and for any elongation in the round ligament. Specimens from the femoral head and acetabulum were fixed with 10% neutral-buffered formalin, and then decalcified. To examine the cartilage morphology, hematoxylin and eosin staining was used with all specimens.

Statistical analysis was carried out to compare the diameter Mann-Whitney's U test. P value less than 0.05 was considered significant.

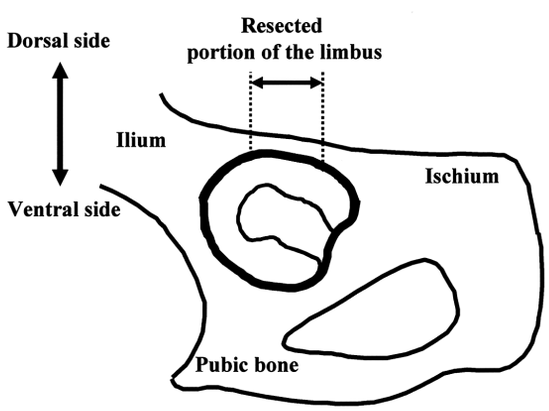


Fig. 1. Limbectomy was performed at the dorsal limbus of the lord-bearing portion. This shows the right hip joint excluding the femoral head.

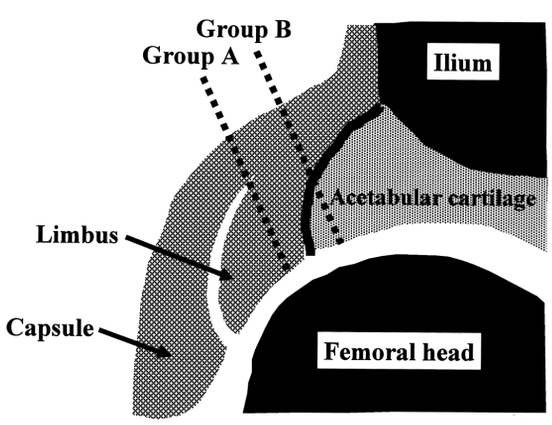


Fig. 2. Coronal view of the hip joint (right side) showing. According to the presence or absence of injury to the acetabular cartilage, the monkeys were divided into the two groups: Group A with simple limbectomy, and Group B with limbectomy and cartilage excision.

RESULTS

The portion of resected the limbus was healed in both groups with hypertrophy, which is the lord bearing side. No hypertrophic change was seen in any other site. Degenerative changes including wear and/or color change and hypertrophy in the joint capsule were noted in all of Group B, and in none of Group A. Flattened deformity in the femoral head was noted in one of Group B. No elongation in the round ligament of the femur was seen in both groups. The details are given in Table 1, and representative photographs are shown in Fig. 3.

The diameter of the acetabulum was significantly enlarged in Group B (longitudinal diameter: $p<0.05$, transverse diameter: $p<0.01$), compared with Group A and controls.

Histologically, the injured limbus was healed with irregular and sparse fibrous tissue in both groups.

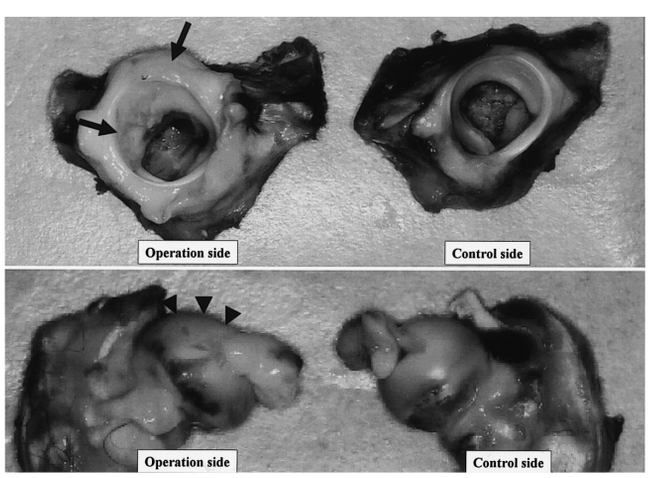


Fig. 3. Extirpated hip joints in Group B. Circular hypertrophy in the joint capsule and a flattened femoral head are observed, compared with the contralateral side.

TABLE 1.
Details of Macroscopic Findings in both Groups

	Healing of injured limbus	Hypertrophy of the joint capsule	Degeneration of the acetabular cartilage	Degeneration of the articular cartilage of the femoral head	Flattened deformity of the femoral head	Elongation of the round ligament of the femur
Group A						
Monkey. 1	+	−	−	−	−	−
Monkey. 2	+	−	−	−	−	−
Monkey. 3	+	−	−	−	−	−
Monkey. 4	+	−	−	−	−	−
Monkey. 5	+	−	−	−	−	−
Group B						
Monkey. 1	+	±	+	+	−	−
Monkey. 2	+	+	+	+	−	−
Monkey. 3	+	±	±	±	−	−
Monkey. 4	+	+	+	+	+	−
Monkey. 5	+	+	±	±	−	−

−: none, ±: mild – moderate, +: prominent

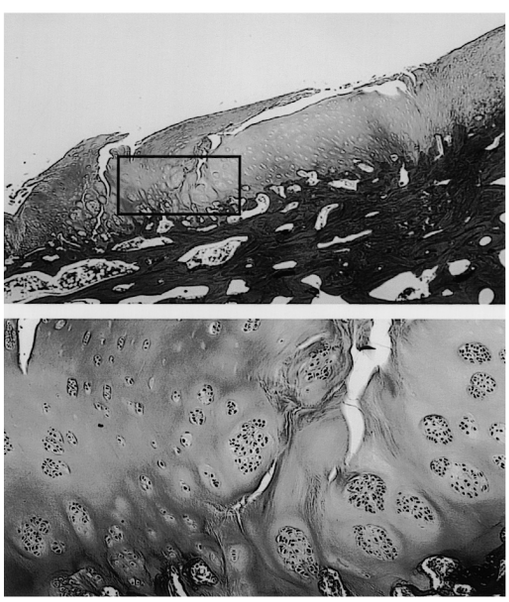


Fig. 4. Microphotographs of acetabular cartilage in Group B. The injured limbus was healed with irregular and sparse fibrous tissue. Fibrillation in the superficial layer of the cartilage and cluster formation were frequently noted.

Fibrillation in the superficial layer of the cartilage and cluster formation were frequently noted in Group B (Fig. 4).

DISCUSSION

Limbectomy in congenital dislocation of the hip has been reported to cause a defect in the anterolateral acetabular cartilage radiologically, possibly due to concomitant cartilage injury [7]. In open reduction of congenital dislocation of the hip, injured acetabular cartilage may lead to poor joint congruity between the femoral head and the acetabulum [8]. These studies suggest that cartilage injury of the acetabulum may result in abnormal growth of the acetabulum. However, whether or not simple limbectomy causes secondary degenerative changes in the involved hip joint has not been yet clarified.

In an animal experimental study, acetabular dysplasia and femoral head deformity occurred subsequent to both labrum and cartilage injury in the hip joint [9]. After surgical procedures with limbectomy and cartilage resection, the involved hip joint showed subluxation tendency [10]. Animal models in these studies, however, have been exclusively made by limbectomy in combination with cartilage resection. To our knowledge, no animal studies have investigated the influence of simple limbectomy on growth. In the present study, we made two types of model (limbectomy only, and limbectomy with cartilage resection), and prospectively examined the influence of the procedures, using monkey in which the hip joint is similar to that in human.

This study found that simple limbectomy did not affect the development of the acetabulum, but caused secondary changes including degeneration in the cartilage, hypertrophy in the soft tissue and/or osseous enlargement in the acetabulum when the cartilage was

excised. In conclusion, these findings suggest that limbectomy without cartilage injury does not influence the growth of the acetabulum.

ACKNOWLEDGMENTS: We dedicated this paper to the of late Prof. Yoshizuka, 1st Department of Anatomy, Kurume University School of Medicine.

REFERENCES

1. Hollinshead WH. Anatomy for Surgeons: The Back and Limbs. Hoeber-Harper, New York, pp 668-670, 1958.
2. Takechi H, Nagashima H, and Ito S. Intra-Articular Pressure of the Hip Joint outside and inside the Limbus. J Jpn Orthop Assoc 1982; 56:529-536.
3. Terayama K, Takei T, and Nakada K. Joint space of the human knee and hip joint under a static load. Engineering in Medicine 1980; 9:67-74.
4. Severin E. Congenital dislocation of the hip. Development of the joint after closed reduction. J Bone Joint Surg 1950; 32-A:507-518.
5. Somerville EW. Result of Treatment of 100 congenital dislocated hips. J Bone Joint Surg 1967; 49-B:258-267.
6. Azuma H, Itoigawa Y, and Sawa S. Structure of the acetabular rim: A comparison of human being and several experimental animals. Hip Joint 1981; 7:189-194. (in Japanese)
7. J. N. O' Hara. Congenital dislocation of the hip: Acetabular deficiency in adolescence (absence of the lateral acetabular epiphysis) after limbectomy in infancy. J Pediatric Ortho 1989; 9:640-648.
8. Hosomi S. Histological and clinical studies of the acetabular labrum. J Joint Surg 1994; 13:295-301. (in Japanese)
9. Hatakenaka T. An experimental study on the influence of surgical procedures for hip joints in young rabbits. J Jpn Orthop Assoc 1977; 51:569-581. (in Japanese)
10. Ohmori S, Yamamoto K, and Maeyama I. Roentgenographic study on the aging process of the femoral head and acetabulum of the experimental hip dysplasia. J West Jpn Orthop Trauma 1977; 26:221-226. (in Japanese)

Original Contribution

Kurume Medical Journal, 54, 35-40, 2007

Muscle Maintenance by Volitional Contraction against Applied Electrical Stimulation

TAKESHI NAGO, YUICHI UMEZU, NAOTO SHIBA, HIROO MATSUSE, TAKASHI MAEDA, YOSHIHIKO TAGAWA*, KENSEI NAGATA AND JEFFREY R BASFORD**

*Rehabilitation Center, Kurume University, Kurume 830-0011, *Department of Mechanical and Control Engineering, Kyushu Institute of Technology, Kitakyushu 804-8550, Japan and **Department of Physical Medicine and Rehabilitation, Mayo Clinic Rochester, Rochester MN 55905, USA*

Received 3 August 2007, accepted 2 November 2007

Edited by HIROYOSHI INOUE

Summary: Muscle training exercises are needed for muscular endurance during spaceflight. This study was designed to investigate effects of volitional contraction against applied electrical stimulation on the muscular endurance of the proximal upper extremity. Thirteen healthy sedentary men were allocated into two groups. One group participated in a hybrid (HYB) exercise regimen in which the biceps brachii was stimulated as he volitionally extended his elbow, and the triceps brachii was stimulated as the volitionally flexed his elbow. The second group underwent a similar regimen in which the electrical stimulation (ELS) was alternatively delivered to the biceps brachii and then to the triceps brachii with the limb fixed. Forty-second surface electromyography (EMG) recordings at 50% maximum voluntary contraction (MVC) were made as baseline data at just before starting the training regimen, and again conclusion. The median frequency (MF) and mean power frequency (MPF) slopes with time were determined using power spectrum analysis. There were statistical significance only for the triceps in which the MF and MPF slopes in the HYB Group became less negative over the period of study (from −45.7±14.7 and −47.0±8.6%/min at baseline to −36.9±10.7 and −36.8±7.0%/min at the end of training, respectively). The corresponding values for these slopes in the ELS Group showed opposite tends with less marked changes of borderline significance for MF and of statistical significance for MPF. These results suggested that the HYB exercise regimen was capable of producing an improvement in triceps but not biceps brachii.

Key words electric stimulation, exercise, muscle endurance, upper extremity

INTRODUCTION

It is known that muscular strength and endurance decrease during spaceflight [1]. Some muscle training regimen is therefore necessary that is both effective and convenient during spaceflight [2].

Resistance exercises are an effective and economical approach to increasing muscle bulk and strength. Gains in strength of as much as 40-100% over 10-12 weeks of training are common even in people who are sedentary, deconditioned or elderly [3,4]. However, there are times when conditions such as immobilization and the low gravity environment of space flight limit the applicability of resistance training and other approaches become necessary. In space flight, especially, the number of slow twitch fibers considerably decrease [5]. As one countermeasure, neuromuscular electrical stimulation (NMES) could be explored for

Address for corresponding author: Takeshi Nago, M.D., Rehabilitation Center, Kurume University, 67 Asahi-machi, Kurume 830-0011, Japan. Tel: +81-(0)942-31-7568 Fax: +81-(0)942-46-6002 E-mail: nago_takeshi@kurume-u.ac.jp

Abbreviations: ELS, electrical stimulation; EMG, electromyography; FFT, fast fourier transform; HYB, hybrid; MF, median frequency; MPF, mean power frequency; MVC, maximum voluntary contraction; NMES, neuromuscular electrical stimulation; ROM, range of motion; SD, standard deviation.

utilization.

NMES, unfortunately, suffers from a number of limitations among which are recruitment patterns that preferentially favor fast twitch fibers [6] and those muscles located near the stimulating electrodes. Another issue that may be particularly important for training to higher levels of function is that NMES strengthening typically does not utilize the reciprocal limb movements that are involved in the activities of everyday life.

An exercise program that involves volitional muscle contraction by applied electrical stimulation may provide an optional regimen. Such regimen would involve electrically stimulated muscles to provide resistance against volitional contraction of the muscle antagonists [7]. This "hybrid" technique would, thus, incorporate the advantages of reciprocal limb movements and muscle contractions without the need for external stabilization or resistance.

Research has found hybrid exercise as capable as or more effective than conventional weight training alone or NMES alone in increasing muscle bulk and strength [8,9]. No study has yet been performed, however, to evaluate the relative impact of these approaches on the fatigue resistance of the strengthened muscles.

The present study was therefore designed to address this lack, by assessing the effects of a hybrid electrical stimulation-volitional muscle contraction exercise regimen versus conventional NMES, on the endurance in the muscles of the proximal upper extremity.

MATERIALS AND METHODS

The IRBs of Kurume University and the Japanese National Space Development Agency approved the clinical design of this study protocol. Following approval, informed consent was obtained from a convenience sample of 13 healthy self-identified right hand dominant sedentary men (age, 22.3±2.3 standard deviation (SD) yr; height, 168.9±5.3 cm; and weight, 64.9±8.8 kg) who had reviewed the goals of the study and agreed to participate. Subjects were required to have normal musculoskeletal examinations and histories; right hand dominance in accordance with the Edinburgh Inventory [10]. Subjects meeting the above criteria were then randomized into two groups matched in age, in weight, and in height. One group, the Hybrid (HYB) exercise Group (HYB, n=7) participated in a combined electrical stimulation-volitional contraction exercise program and the other, the electrical stimulation (ELS) Group (n=6), took part in a conventional (isometric) NMES program.

Exercise

Subjects trained 3 times a week for 8 weeks. Each exercise session consisted of the participant lying supine and voluntary or electrically performing 10 sets of 10 reciprocal elbow flexion and extension contractions with their non-dominant left upper extremity. Contractions were 2 sec in duration and sets were separated by 1-min rest intervals. An exercise session required 15 min and 40 sec to complete.

HYB Group: Exercises were performed in the supine position with the subject's biceps brachii stimulated as the volitionally extended the elbow; the reverse occurred (i.e., the triceps brachii was stimulated) as the volitionally flexed their elbow [9]. The range of motion (ROM) of the joint was measured using a goniometer, and was restricted to an arc that extended from 15 to 105° elbow flexion. The subject changed the direction of his muscle contractions, in accordance with a tone emitted by the stimulator.

ELS Group: Subjects in this group also lay supine in the manner described above. The procedures and the number of session were identical as in the HYB Group with the exception that the subjects were each instructed to avoid volitional contraction of the muscle and the left elbow was immobilized in a brace at 60° flexion.

Equipment: The HYB training apparatus consisted of an electrical stimulator, surface electrodes, and a joint motion sensor that triggered stimulation of the antagonist once it sensed the initiation of a volitional contraction [9]. Low impedance gel-coated electrodes (Sekisui Plastics Co., Tokyo, Japan) placed over the motor points of the biceps and triceps brachii have been previously described [7,9].

Stimulation parameters

Waveform: Stimulation parameters were based on a standard Russian waveform in which a 5 kHz carrier frequency was modulated at 20 Hz (2.4 ms on, 47.6 ms off) to deliver rectangular biphasic wave pulses [7].

Intensity: Stimulation intensities were set at the value of the threshold intensity plus two-thirds the difference between the maximum comfortable intensity and the threshold intensity [7-9], with the isometric contraction force limited to 25-30% of the maximum voluntary contraction (MVC). Output power was <10W, the current intensity was <10 mA/cm^2, and the voltage was <80V.

Evaluation

Strength: Muscle strength of each subject was evaluated one week before the regimen as a baseline and also evaluated one week after the regimen for an endpoint. Subjects were each evaluated during a baseline session that was undertaken within one week prior to his entering the study protocol, as well as during the one week after the end of the program. Maximal isometric elbow flexion and extension torques were obtained with the subject sitting in a Kin-Com apparatus (Chattanooga Group, Inc., TN, USA) with the left elbow positioned at 60° flexion. Each subject was then asked to produce a maximal isometric elbow flexion and extension and encouraged to monitor his own efforts on a video screen. The maximum voluntary contraction was defined as the mean of three measurements at 1-min intervals.

Endurance: Muscle fatigue was assessed in a standardized manner. Since a >40% MVC is reported to be necessary for successful surface electromyography (EMG) power density spectral analysis of fatigue in the upper extremities [11], we chose to perform testing at 50% MVC. A consistent procedure was followed which began with the subject first sitting in a relaxed manner for 2-3 min and then performing a preliminary/training series of 40-sec isometric elbow flexion and extension contractions at the 50% MVC in the manner described in the strength determination section above. Isometric endurance testing of elbow flexion and extension were then performed with video feedback in a manner similar to that of the training sessions. The duration of each session was more than 15 min, after having measured the flexion and measured the extension.

EMG recording: The skin over the bellies of the left biceps and triceps brachii was first cleansed with an alcohol swab. Next, a pair of 10-mm-diameter 20-mm-center-to-center separation silver-silver chloride bipolar surface electrodes was placed over the motor end-points of each of the two muscles. The biceps and triceps EMG activities were continuously monitored during their respective 40-sec testing durations. The EMG signals were amplified, digitized at a sampling rate of 2000 Hz, and stored on memory cards in an ME 3000P EMG analysis system (Mega Electronics, Ltd, Helsinki, Finland). Records were downloaded and analyzed off-line using the manufacturer's proprietary software (MegaWin software 2006 version 2.0, Mega Electronics, Ltd, Helsinki, Finland). The EMG preamplifier sensitivity was set at 1 μV, and the frequency bandwidth at 20-500 Hz.

Evaluation of muscle fatigue: EMG power spectral frequency analysis was used to evaluate skeletal muscle endurance [12-20]. The median frequency (MF) and the mean power frequency (MPF) indices were derived from the raw EMG signals and plotted against time using the ME3000P Fast Fourier Transform (FFT) spectral analysis program. The MF and MPF slopes per unit time over the 40-sec 50%-MVC elbow flexion and extension testing periods were calculated from the following formula: % slope=[(final frequency – initial frequency)/time]×100. The values were normalized and expressed as a percentage of the individual's baseline prior to further analysis and comparison between the groups.

Data analysis

Statistical analyses were performed with Stat-View, Version 5.0, for Windows (SAS, Cary, NC, USA). Data were expressed as mean ± standard deviation (SD). Changes in MF and MPF spectral frequency distributions during the 40-sec isometric contraction tests were assessed using the Pearson's product moment correlation test. Inter-group differences between the MF and MPF slopes in the HYB and ELS Groups were examined for statistical significance using Student's unpaired t-test. Intra-group changes in each parameter between their baseline and endpoint determinations were examined for statistical significance using Student's paired t-test. A P-value at less than 0.05 was considered to denote statistical significant.

RESULTS

The groups were matched and did not differ in a statistically significant manner in terms of age, height, and weight. All the 13 subjects attended and completed all the training and evaluation sessions.

Spectral power analysis

The slopes of MF and MPF decreased linearly between the baseline and endpoint period in elbow flexion and extension endurance testing sessions in all subjects (by Pearson's product moment correlation coefficient) (in all cases $p<0.01$).

The baseline MF and MPF slopes in the biceps during elbow flexion did not statistically differ between the groups ($p=0.19$, and $p=0.43$, respectively). Intra-group analysis among the HYB Group revealed nosignificant changes between the baseline values (MF −32.9±5.3, and MPF −33.3±6.8%/min) and the values at the end of training (MF −40.0±21.9, and MPF −38.2±13.9%/min) ($p=0.40$, and $p=0.45$, respec-

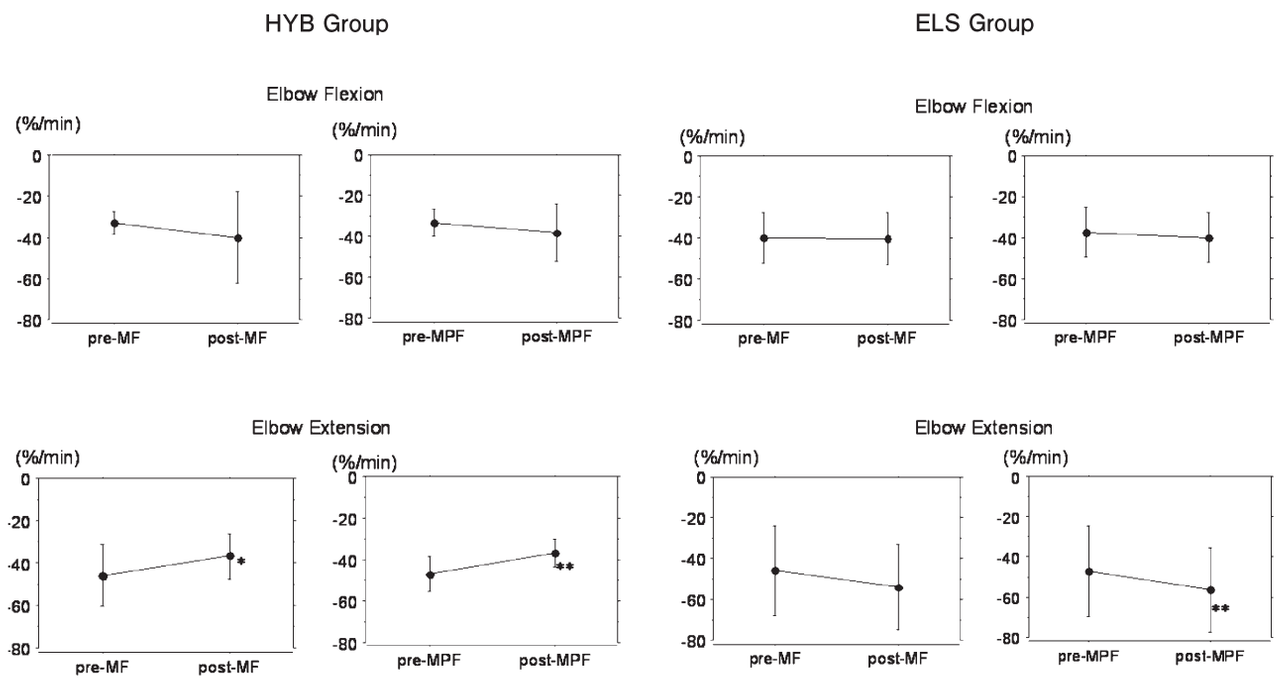


Fig. 1. Left Panels. HYB group. Comparison of MF and MPF slopes (means ± SD) of the biceps during elbow flexion and triceps during extension before (pre) and after (post) four weeks of HYB training. While training had no effect on the MF (p=0.40) or MPF (p=0.45) slopes of the biceps, it did produce statistically significant improvements in both of these quantities in the triceps (*MF: p=0.03, **MPF: p<0.01). Right Panels. ELS group. Comparisons of MF and MPF slopes (means ± SD) of the biceps during elbow flexion and the triceps during extension before (pre) and after (post) four weeks of ELS training. While training had no effect on biceps MF and MPF slopes during elbow flexion (MF: p=0.95, MPF: p=0.60) it did produce a statistically significant worsening of the MPF slope (p<0.01) and a borderline worsening in the MF slope (p=0.054) during elbow extension.

tively) (Fig. 1, Upper Left). Intra-group analysis of the ELS Group revealed a similar pattern of no significant difference between the baseline values (MF −39.9±12.3, and MPF −37.7±12.1%/min) were statistically indistinguishable from those recorded at the end of training (MF −40.3±12.6, and MPF −39.9±12.1%/min) (p=0.95, and p=0.60, respectively) (Fig. 1, Upper Right). Analysis revealed that these nonsignificant intra-group changes were accompanied by similar nonsignificant inter-group changes (MF p=0.97, MPF p=0.80).

The baseline values of the MF and MPF slopes in the triceps during elbow extension did not differ between the groups in a statistically significant manner at baseline (p= 0.95, and p= 0.99, respectively). These slopes improved following training in the HYB Group (from −45.7±14.7 and −47.0±8.6%/min at baseline to −36.9±10.7 and −36.8±7.0%/min at the end of training) (p=0.03, and p<0.01, respectively) (Fig. 1, Lower Left). The corresponding values for these slopes in the ELS Group however became steeper following training (from −46.8±21.8 and −47.1±22.4%/min, to −54.0±21.2 and −56.4±21.1%/min) with change in MF slope approaching (p=0.054) significance and that in MPF slope showing statistical significance (p<0.01) (Fig. 1, Lower Right). Inter-group comparison between the HYB Group and the ELS Group demonstrated these findings in changes improved muscular endurance in the triceps in the HYB Group relative to the changes in the ELS Group (p<0.05).

DISCUSSION

The findings from this study indicated that while a HYB exercise regimen resulted in an improvement in the resistance of the triceps to fatigue (as determined from MF and MPF slopes). Training with a comparable electrical stimulation strengthening regimen has been associated with a decrease in triceps endurance. The present study found that neither the HYB nor the ELS training had a beneficial effect on the resistance of the biceps to muscular fatigue.

The discrepancy between the responses in the training in the biceps and triceps is intriguing as the

two muscles were stimulated at the same relative intensity (threshold intensity + 2/3rds the difference between the maximum comfortable intensity and the threshold intensity). It is possible that the reason for the difference may lie in the different fiber composition of the two muscles: the triceps has a higher proportion of slow twitch fibers than the biceps in monkey [21,22], and at least one recent report has suggested that gains in strength by electrical stimulation in fast twitch rich muscles comes at a cost of decreased endurance in human lower extremities [17]. The finding that the fatigue resistance of the triceps in the HYB Group improved with training while that of the ELS Group worsened may have a similar root cause. Elder reported in human that while the medial head of triceps was found to be mainly composed of slow twitch fibers, fast twitch fibers were found to be more prevalent than slow twitch fibers in the lateral and long heads of triceps as well as the biceps brachii using fresh cadaver [23]. The opinion of researchers varies by their specimens or subjects, and it is difficult to arrest these results equally. Further study should be necessary to determine on the fiber distribution.

Also, it is possible that the reason for the difference may lie in the different strength of the two muscles: the maximal elbow extension torques were bigger than the maximal elbow flexion torques [7,9]. Muscular strength training requires an exercise load of strong intensity; on the other hand, muscular endurance training requires an exercise load of low intensity [24]. I believe that because the electrically stimulated eccentric contraction preferentially recruits fast twitch fibers, the concentric contraction of the HYB regimen contributes to improve muscular endurance. For muscular endurance improvement, in this study, the concentric exercise load for the triceps might be appropriate, but for the biceps might be too big. Kramer [25] reported the male subjects demonstrated significantly greater electrically stimulated knee extension torque values as well as maximal voluntary knee extension torque values than did the female subjects. It would be necessary in muscle maintenance to regulate electrical stimulation intensity to each muscle.

Using MF and MPF slopes as a measure for muscular endurance deserves some discussion. The choice may be arguable but seems appropriate as physiological research confirms an association between muscle fatigue and shifts in firing rates towards lower values [7,12-20]. Moreover, regression analyses between the MF and MPF slopes with time were capable of detecting differential responses in the fiber types: with slow twitch fibers showing more resistance to fatigue than the fast twitch fibers [26,27].

Another concern involves the spectral analysis for the upper extremities: other reports have examined the muscles of the back and lower extremities. However, studies on the muscle in the upper extremities also appear in the literature. For example, an investigation by members of this group found that the MF and MPF slopes in the triceps brachii of wheelchair marathoners displayed an improved endurance relative to wheelchair naïve ambulatory control subjects [20]. It is also significant that another recent upper extremity study [28] has revealed that the fast twitch fiber rich biceps reveals a steeper degradation in its firing frequency than the slow twitch rich triceps [21,22,26].

HYB regimen was capable of producing an improvement in the muscular endurance of the triceps brachii, however, the changes in fiber type by HYB approach inconclusive in this study. Further research is necessary to investigate the improvement of muscular strengthening and endurance on other muscles as well as change in their fiber types. We also hope to continue the study of the long-term effects of this exercise, and to refine the HYB approach.

CONCLUSIONS

Our HYB exercise regimen was capable of producing an improvement, and conventional electrical stimulation of worsening, in the muscular endurance of the triceps brachii. Neither approach, however, appears to have a significant effect on the fatigue resistance of the biceps brachii.

REFERENCES

1. Jaweed MM. Muscle Structure and Function. In: Space Physiology and Medicine, eds. Nicogossian AE, Huntoon CL, Pool SL, Lea & Febiger, Malvern, pp 317-326, 1994.
2. Nicogossian AE, Sawin CF, and Grigoriev AI. Countermeasures To Space Deconditioning. In: Space Physiology and Medicine, eds. Nicogossian AE, Huntoon CL, Pool SL, Lea & Febiger, Malvern, pp 447-467, 1994.
3. Fiatarone MA, O'Neill EF, Ryan ND, Clements KM, Solares GR et al. Exercise training and nutritional supplementation for physical frailty in very elderly people. N Engl J Med 1994; 330:1769-1775.
4. Rall LC, Meydani SN, Kehayias JJ, Dawson Hughes B, and Roubenoff R. The effect of progressive resistance training in rheumatoid arthritis. Increased strength without changes in energy balance or body composition. Arthritis Rheum 1996; 39:415-426.
5. Edgerton VR, Zhou MY, Ohira Y, Klitgaard H, Jiang B et al. Human fiber size and enzymatic properties after 5 and 11 days of spaceflight. J Appl Physiol 1995; 78:1733-1739.

6. Chilibeck PD, Bell G, Jeon J, Weiss CB, Murdoch G et al. Functional electrical stimulation exercise increases GLUT-1 and GLUT-4 in paralyzed skeletal muscle. Metabolism 1999; 48:1409-1413.
7. Yanagi T, Shiba N, Maeda T, Iwasa K, Umezu Y et al. Agonist contractions against electrically stimulated antagonists. Arch Phys Med Rehabil 2003; 84:843-848.
8. Iwasaki T, Shiba N, Matsuse H, Nago T, Umezu Y et al. Improvement in Knee Extension Strength through Training by Means of Combined Electrical Stimulation and Voluntary Muscle Contraction. Tohoku J Exp Med 2006; 209:33-40.
9. Matsuse H, Shiba N, Umezu Y, Nago T, Tagawa Y et al. Muscle training by means of combined electrical stimulation and volitional contraction. Aviat Space Environ Med 2006; 77:581-585.
10. Oldfield RC. The assessment and analysis of handedness: the Edinburgh inventory. Neuropsychologia 1971; 9:97-113.
11. Bernardi M, Solomonow M, and Baratta RV. Motor unit recruitment strategy of antagonist muscle pair during linearly increasing contraction. Electromyogr Clin Neurophysiol 1997; 37:3-12.
12. Clark BC, Manini TM, Thé DJ, Doldo NA, and Ploutz-Snyder LL. Gender differences in skeletal muscle fatigability are related to contraction type and EMG spectral compression. J Appl Physiol 2003; 94:2263-2272.
13. Dousset E, and Jammes Y. Reliability of burst superimposed technique to assess central activation failure during fatiguing contraction. J Electromyogr Kinesiol 2003; 13:103-111.
14. Gayda M, Merzouk A, Choquet D, and Ahmaidi S. Assessment of skeletal muscle fatigue in men with coronary artery disease using surface electromyography during isometric contraction of quadriceps muscles. Arch Phys Med Rehabil 2005; 86:210-215.
15. Kleine BU, Schumann NP, Stegeman DF, and Scholle HC. Surface EMG mapping of the human trapezius muscle: the topography of monopolar and bipolar surface EMG amplitude and spectrum parameters at varied forces and in fatigue. Clin Neurophysiol 2000; 111:686-693.
16. Koumantakis GA, Oldham JA, and Winstanley J. Intermittent isometric fatigue study of the lumbar multifidus muscle in four-point kneeling: an intra-rater reliability investigation. Man Ther 2001; 6:97-105.
17. Marqueste T, Hug F, Decherchi P, and Jammes Y. Changes in neuromuscular function after training by functional electrical stimulation. Muscle Nerve 2003; 28:181-188.
18. McHugh MP, Tyler TF, Nicholas SJ, Browne MG, and Gleim GW. Electromyographic analysis of quadriceps fatigue after anterior cruciate ligament reconstruction. J Orthop Sports Phys Ther 2001; 31:25-32.
19. Umezu Y, Kawazu T, Tajima F, and Ogata H. Spectral electromyographic fatigue analysis of back muscles in healthy adult women compared with men. Arch Phys Med Rehabil 1998; 79:536-538.
20. Umezu Y, Shiba N, Tajima F, Mizushima T, Okawa H et al. Muscle endurance and power spectrum of the triceps brachii in wheelchair marathon racers with paraplegia. Spinal Cord 2003; 41:511-515.
21. Chopard A, Leclerc L, Pons F, Leger JJ, and Marini JF. Effects of 14-day spaceflight on myosin heavy chain expression in biceps and triceps muscles of the rhesus monkey. J Gravit Physiol 2000; 7:47-49.
22. Roy RR, Bello MA, Powell PL, and Simpson DR. Architectural design and fiber-type distribution of the major elbow flexors and extensors of the monkey (cynomolgus). Am J Anat 1984; 171:285-293.
23. Elder GC, Bradbury K, and Roberts R. Variability of fiber type distributions within human muscles. J Appl Physiol 1982; 53:1473-1480.
24. Ishii N. Factors involved in the resistance exercise stimulus and their relations to muscular hypertrophy. In: Exercise, Nutrition and Environmental Stress, eds. Nose H, Spriet LL, Imaizumi K, Cooper, MI, pp 119-138, 2002.
25. Kramer JF. Effect of electrical stimulation current frequencies on isometric knee extension torque. Phys Ther 1987; 67:31-38.
26. Kupa EJ, Roy SH, Kandarian SC, and De Luca CJ. Effects of muscle fiber type and size on EMG median frequency and conduction velocity. J Appl Physiol 1995; 79:23-32.
27. Merletti R, and Roy S. Myoelectric and mechanical manifestations of muscle fatigue in voluntary contractions. J Orthop Sports Phys Ther 1996; 24:342-353.
28. Krivickas LS, Taylor A, Maniar RM, Mascha E, and Reisman SS. Is spectral analysis of the surface electromyographic signal a clinically useful tool for evaluation of skeletal muscle fatigue? J Clin Neurophysiol 1998; 15:138-145.

Original Contribution

Kurume Medical Journal, 54, 41-49, 2007

Clinicopathological Study of Patients Undergoing Resection of Hilar Cholangiocarcinoma

ATSUHIRO HIDAKA

Department of Surgery, Kurume University School of Medicine, Kurume 830-0011, Japan

Received 20 September 2007, accepted 20 November 2007

Summary: Of the patients who underwent resection of hilar cholangiocarcinoma, those who received palliative surgery, or could not be followed up clinicopathologically, were excluded from this study. In the remaining 37 patients, the cumulative postoperative survival rate (simply referred to as the cumulative survival rate below) was analyzed according to gross types, histopathological parameters, final stages, and final curability. These patients showed a 5-year survival rate of 17.7% and a 50% survival of 2.2 years. By gross type, patients with a localized papillary or nodular expansion type tended to have a better survival rate than those with an invasive papillary or nodular expansion type. A greater histological depth of invasion tended to be associated with a poorer prognosis: the s(−) group, that is, a group of patients without serosal exposure of cancer (invasion depths of m, fm, and ss) had a significantly better prognosis than the s(+) group, a group of patients with serosal exposure of cancer (invasion depths of se and si). Other histopathological parameters, such as ly, pn, pHinf, pHM, and pEM, were associated with significant prognostic differences. By final stage, the stage I/Ⅱ group and stage Ⅲ or higher group showed a particularly significant difference in prognosis. By final curability, the curability A/B group had a significantly better prognosis than the curability C group. Taken together, surgery providing curability A and B promises a good long-term prognosis. Therefore, it is important that efforts are made to detect cancer early, adequately evaluate the degree of cancer extension, and determine the extent of resection and the surgical technique.

Key words hilar cholangiocarcinoma, cumulative survival rate, histopathological parameter, final stage, final curability

INTRODUCTION

Recent advances in diagnostic imaging techniques and perioperative management have been improving treatment results in cholangiocarcinomas. However, many hilar cholangiocarcinomas cannot be radically resected because of their state of extension. Even if they are resectable, their long-term prognosis is far from satisfactory. The accurate preoperative staging of cholangiocarcinomas and their reliable resection based on surgical anatomy are important. In this study, we clinicopathologically analyzed patients who had undergone resection of hilar cholangiocarcinoma in our department, and determined conditions for achieving long-term survival.

MATERIALS AND METHODS

Sixty-three patients had undergone resection of hilar cholangiocarcinoma in Kurume University Hospital between 1997 and 2003. In those, 37 patients were studied, excluding those who received palliative surgery (16 patients), or could not be followed up clinicopathologically (10 patients). They consisted of 20 men

Address for corresponding author: Atsuhiro Hidaka M.D., Department of Surgery, Kurume University School of Medicine, 67 Asahi-machi, Kurume 830-0011, Japan. Tel: 0942-31-7567 Fax: 0942-35-8967 E-mail: atushiro@st-mary-med.or.jp

Abbreviations: PTBD, percutaneous transhepatic biliary drainage; PTCS, percutaneous transhepatic cholangioscopy; PTPE, percutaneous transhepatic portal embolization.

TABLE 1.
Breakdown of surgical techniques

Surgical technique	Number of patients	Caudate lobectomy	Concomitant vascular resection	Pancreaticoduodenectomy
Left hepatic lobectomy	8	6	1	0
Extended left hepatic lobectomy	6	2	4	0
Right hepatic lobectomy	4	2	0	1
Extended right hepatic lobectomy	9	5	1	0
Right hepatic trisegmentectomy	1	0	0	0
S4a+S5 liver segmentectomy	5	0	0	1
Others	4	0	1	2
Total	37	15	7	4

and 17 women, ranging in age from 52 to 77 years, with a mean of 63.7±6.47 years. All patients had undergone hepatectomy with extrahepatic bile duct resection (Table 1). Cumulative postoperative survival rates were compared among gross types, clinicopathological parameters, final stages, and final curability. Positive and negative groups were defined by scores of 0 and 1 or higher, respectively, for ly, v, pn, pHinf, pGinf, and pN. Negative and positive resection margins were defined by a score of 0 or 1 and that of 2, respectively, for pHM, pDM, and pEM. Because of the small number of combined resections, cumulative postoperative survival rates were not compared among pPanc, pDu, pPV, and pA. Pathological examination was performed according to the General Rules for Surgical and Pathological Studies on Cancer of the Biliary Tract by the Japanese Society of Biliary Surgery [1]. Survival curves by parameters were calculated by the Kaplan-Meier method. The significance of differences was analyzed by the log rank test. Multivariate analysis was performed by using cluster analysis. P values less than 0.05 were considered significant.

RESULTS

The patients had overall 3- and 5-year survival rates of 28.2% and 17.7%, respectively (Fig. 1), and a 50% survival time of 2.2 years.

Survival rates by gross type

Cancers were classified into localized and invasive papillary or nodular expansion types. The 3- and 5-year survival rates of patients with localized types were both 33.3%, whereas the 3- and 5-year survival rates of those with invasive types were 27.4% and 15.6%, respectively. The invasive types tended to lead to better survival rates than their localized counterparts, with no significant differences.

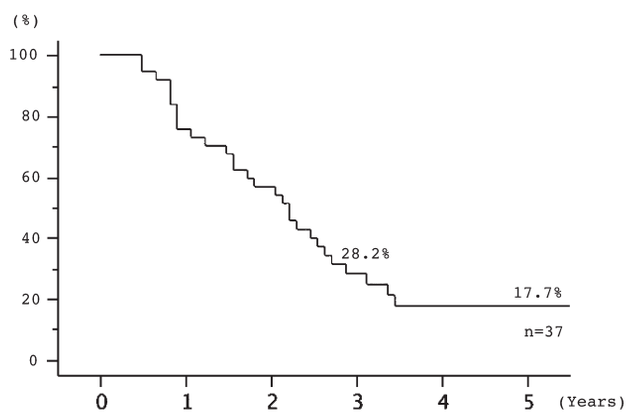


Fig. 1. Survival rates in resected patients with hilar cholangiocarcinoma.

Survival rates by histological type

Thirty-six cancers were analyzed, excluding 1 of unknown histopathology (no histopathological record). Cancers were divided into well-differentiated papillary (pap) and tubular adenocarcinomas (tubl) and other histological types. The 3- and 5-year survival rates in the well-differentiated types were 37.9% and 25.2%, respectively, and the 3-year survival rate in other histological types was 18.8%. The well-differentiated types tended to lead to a better survival rate, with no significant difference from that in the other types.

Survival rates by histological depth of cancer invasion

A greater depth of invasion tended to be associated with a poorer prognosis. The 3- and 5-year survival rates were 55.0% and 45.8%, respectively, in the s(−)

group, that is, a group without serosal exposure of cancers with invasion depths of m, fm, and ss, and 11.6% and 0%, respectively, in the s(+) group with serosal exposure of cancers with invasion depths of se and si. Thus, the prognosis was significantly better in the s(−) group (Fig. 2).

Survival rates by the presence or absence of neurovascular invasion

Lymphatic invasion (ly): Thirty-six cancers were analyzed, excluding 1 of unknown histopathology. The 3- and 5-year survival rates in the ly(−) group were significantly higher, both at 68.6%, than 20.1% and 8.1%, respectively, in the ly(+) group.

Venous invasion (v): Twenty-nine cancers were analyzed, excluding 8 of unknown histopathology. The 3- and 5-year survival rates in the v(−) group tended to be higher, but not significantly, both at 53.6%, than 26.5% and 10.6%, respectively, in the v(+) group.

Neural invasion (pn): Thirty-six cancers were analyzed, excluding 1 of unknown histopathology. The 3- and 5-year survival rates in the pn(−) group were significantly higher, both at 71.4%, than 17.9% on the 3-year survival rate in the pn(+) group.

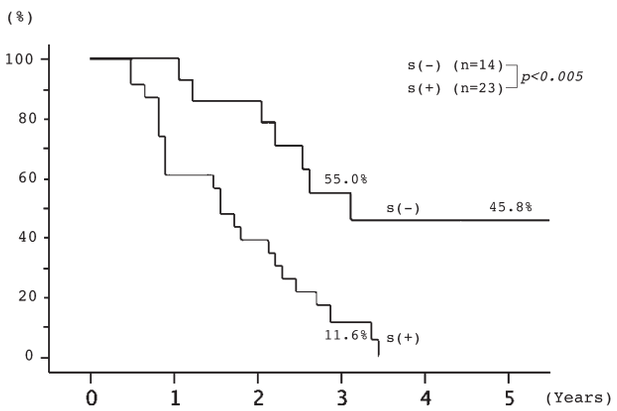


Fig. 2. Survival rates by histological depth of invasion.

Survival rates by the presence or absence of histological invasion of other organs (extension to the surrounding tissue)

Direct intrahepatic invasion (pHinf): Thirty-three cancers were analyzed, excluding 4 of unknown histopathology. The 3- and 5-year survival rates in the pHinf(−) group were significantly higher, at 43.6% and 34.9%, respectively, than 16.7% on the 3-year survival rate in the pHinf(+) group.

Gallbladder-side invasion (pGinf): Thirty-six cancers were analyzed, excluding 1 of unknown histopathology. The 3- and 5-year survival rates in the pGinf(−)

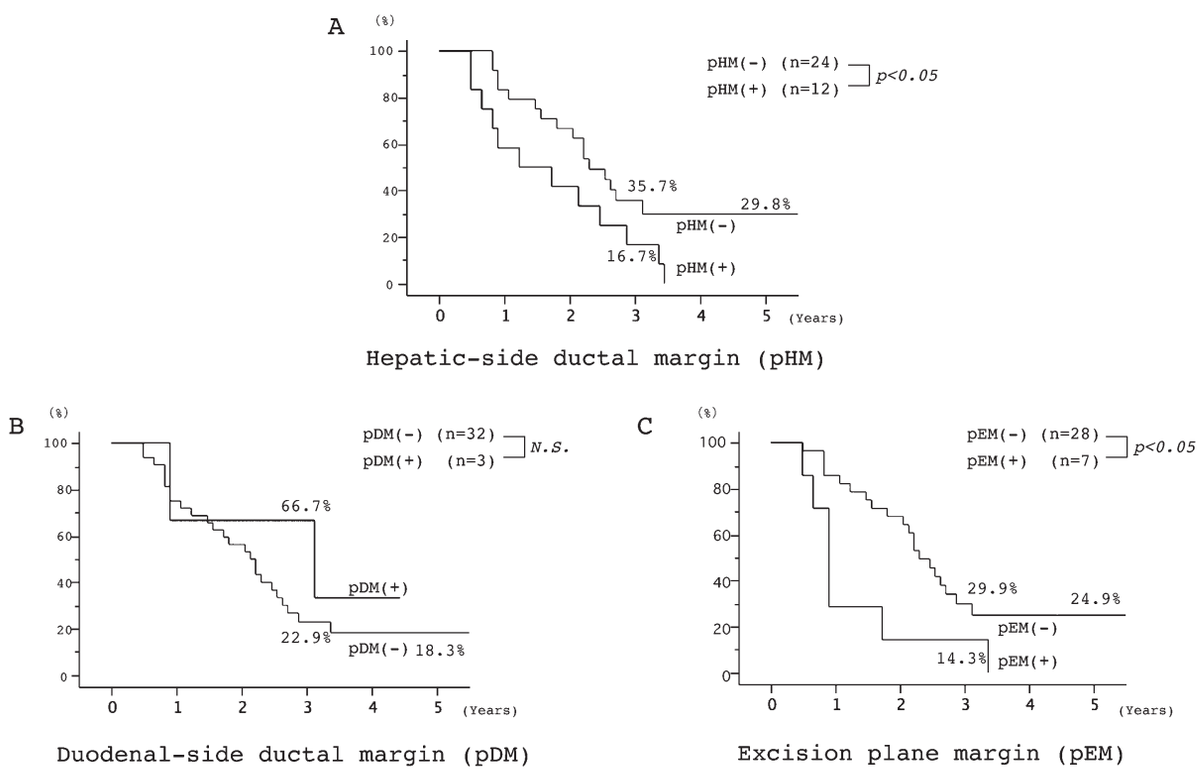


Fig. 3. Survival rates by parameters related to the resection margin.

group tended to be higher, but not significantly, at 34.7% and 27.8%, respectively, than 18.2% and 0%, respectively, in the pGinf(+) group.

Survival rates by the presence or absence of lymph node metastasis

Thirty-five cancers were analyzed, excluding 2 of unknown histopathology. The 3- and 5-year survival rates in the pN(−) group tended to be higher, but not significantly, at 35.4% and 28.3%, respectively, than 21.4% and 7.1%, respectively, in the pN(+) group.

Survival rates by the presence or absence of histological residual cancer in the resection margin

Hepatic-side ductal margin (pHM): Thirty-six cancers were analyzed, excluding 1 of unknown histopathology. The 3- and 5-year survival rates in the pHM(−) group were significantly higher, at 35.7% and 29.8%, respectively, than 16.7% and 0%, respectively, in the pHM(+) group (Fig. 3A).

Duodenal-side ductal margin (pDM): Thirty-five cancers were analyzed, excluding 2 of unknown histopathology. The 3- and 5-year survival rates in the pDM(−) group were 22.9% and 18.3%, respectively, and the 3-year survival rate in the pDM(+) group was 66.7%. No difference was noted in the survival rate (Fig. 3B).

Excision plane margin (pEM): Thirty-five cancers were analyzed, excluding 2 of unknown histopathology. The 3- and 5-year survival rates in the pEM(−) group were significantly higher, at 29.9% and 24.9%, respectively, than 14.3% and 0%, respectively, in the pEM(+) group (Fig. 3C).

Survival rates by final stage

Significant differences were noted among cumulative survival rates by final stage; in particular, the difference was marked between the stage I+II group and

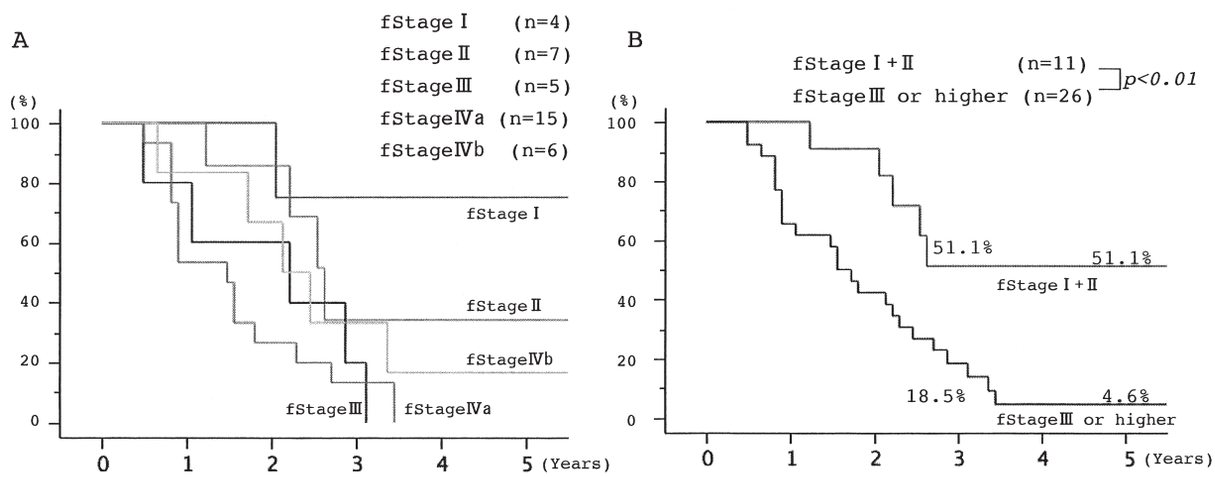


Fig. 4. Survival rates by final stage.

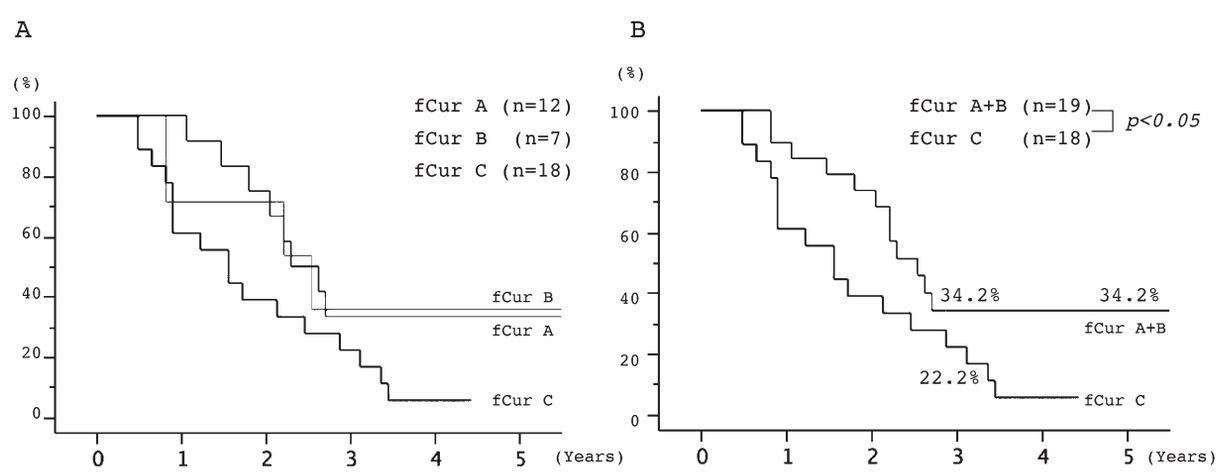


Fig. 5. Survival rates by final curability.

the stage Ⅲ or higher group (Fig. 4). The 3- and 5-year survival rates were both 51.5% in the final stage I/Ⅱ group, and 18.5% and 4.6%, respectively, in the final stage Ⅲ or higher group.

Survival rates by final curability

The final curability A/B group had a significantly better prognosis than the final curability C group (Fig. 5). The 3- and 5-year survival rates were both 34.2% in the final curability A/B group, and the 3-year survival rate was 22.2% in the final curability C group.

DISCUSSION

History of surgical treatment of hilar cholangiocarcinoma

Hilar cholangiocarcinoma has attracted attention under the name of Klatskin tumor [2], since Klatskin [3] reported in 1965 that cancers in this location frequently caused fatal hepatic failure despite their small size and slow growth with infrequent metastasis. Since hilar cholangiocarcinomas are in an anatomically complex location, radical surgery is difficult to perform despite their small size, and they have been generally regarded as tumors that are anatomically difficult to treat [4]. Later, the anatomy of the hepatic hilum was gradually clarified [5-7], and aggressive resection including hepatectomy came to be performed [8-11]. The history of surgical treatment began in 1954 with Brown's success in the two-stage resection of the extrahepatic bile duct [12]. However, the so-called Longmire's operation [13] (involving internal fistulation by left intrahepatic cholangiojejunostomy) and the report of Terblanche et al. [14] that bypass surgery alone without local resection achieved long-term survival may have discouraged surgeons against trying surgical resection in the 1970s. The surgical technique of Cameron et al. [15] involving local bile duct resection followed by cholangiojejunostomy and percutaneous silicon tube stenting promoted resection therapy to some extent. Hart and White [16] developed a surgical technique in which a good visual field was ensured for adequate resection and reconstruction of the bile duct by resecting the anterior liver parenchyma at the hepatic hilum, the so-called inferior portion (S4a) of the medial segment of the left liver lobe. This was a step forward to approach the difficult-to-reach hilar bile duct. However, as was clarified by later studies of the local anatomy of the hepatic hilum, their resection technique inevitably left cancer behind in the resection margin. On the other hand, an attempt at radical tumor resection by hepatic lobectomy began in 1962 with left hepatic lobectomy by Altemeier [17]. In 1964, Quattlebaum first tried right hepatic lobectomy [18], in which Bird et al. first succeeded in 1969 [19]. In the latter 1960s, Haynes et al. [20] and Cady and Fortner [21] reported successful left hepatic lobectomy. In the 1970s, cases of successful left hepatic lobectomy were reported in succession. In 1973, Longmire et al. [22] succeeded in combined right hepatic trisegmentectomy and portal vein resection with end-to-end anastomosis reconstruction. In 1976, Fortner et al. [23] succeeded in left hepatic lobectomy followed by heterotopic liver transplantation, and the patient survived for 8 months. From 1980 onwards, many reports were published from Japan as well as from Europe and the United States, and the number of cases of combined portal vein and liver resection increased yearly, as reported by Tsuzuki et al. [24], Sakaguchi et al. [25], and Nimura et al. [26]. Caudate lobectomy is another important surgical factor in performing radical surgery for hilar cholangiocarcinoma. Blumgart et al. [27] first described concomitant caudate lobectomy in 1979, but did not clearly state the rationale for it. Later, Japanese researchers, Tsuzuki et al. [24], Mizumoto et al. [28], Iwasaki et al. [29], and Nimura et al. [30] successively published clinical study reports, and studies have demonstrated in more detail the clinically oriented local anatomy of the hepatic caudate lobe and the surgical anatomy of intrahepatic bile duct branches and the hepatic hilum [31-37], achieving a worldwide consensus about the rationality of caudate lobectomy in surgery for hilar cholangiocarcinoma [38,39]. In our department, we have performed concomitant caudate lobectomy in only 15 (40.5%) of the 37 patients to date. However, Mizumoto et al. [40] pointed out the importance of caudate lobectomy for hilar cholangiocarcinoma in 1984, and further histopathological studies demonstrated the invasion of caudate lobe parenchyma and bile duct branches by hilar cholangiocarcinoma. Therefore, we consider that caudate lobectomy is essential in any surgical technique of hepatectomy performed for hilar cholangiocarcinoma, that is, left hepatic lobectomy, extended left hepatic lobectomy, right hepatic lobectomy, extended right hepatic lobectomy, right hepatic trisegmentectomy, or S4a+S5 liver segmentectomy [41]. Currently, we have a policy to perform concomitant caudate lobectomy whenever possible.

Preoperative management

Jaundice-reducing procedure: In addition to preop-

erative management for general open abdominal surgery, meticulous care is needed particularly to avoid postoperative liver failure in patients with hilar cholangiocarcinoma. Most patients with hilar cholangiocarcinoma present with obstructive jaundice, and US and CT can demonstrate dilatation of some or all intrahepatic bile ducts. In Japan, it is taken for granted that jaundice reduction by percutaneous transhepatic biliary drainage (PTBD) [42] decreases postoperative complications [8,43]. With poor management of jaundice, the operative mortality is reported to be more than 20% [44]. In principle, all segments of the liver except the caudate lobe should be drained by PTBD to perform selective cholangiography necessary for the diagnosis of the degree of cancer extension (described below) and to prevent segmental cholangitis. In performing PTBD, it is essential to puncture a site away from the lesion. PTBD of a bile duct close to the site of biliary stenosis, where a cancer may be present, increases the likelihood of cancer extension or dissemination along the fistula. What is worse, the bile duct near the PTBD catheter insertion site is intensely inflamed, and Glisson's capsules undergo scarring in clumps, making it difficult to image-diagnose the extent of cancer extension. In addition, these changes can be misidentified as cancer during surgery, and the separation from arteries and the portal vein becomes extremely difficult, thereby constituting a serious impediment to performing radical surgery. Therefore, PTBD in the vicinity of the hepatic hilum is virtually contraindicated, and a site well away from the stenosis should be punctured [45].

Management of liver failure: Postoperative liver failure is the most serious postoperative complication of hilar cholangiocarcinoma, and accounts for the majority of postoperative in-hospital deaths [46]. Unlike the normal liver, the obstructive-jaundiced liver has some residual dysfunction even if biliary drainage has been performed for jaundice reduction. Therefore, liver dysfunction may develop after major hepatectomy. Since there is no effective treatment for postoperative liver failure, preoperative prevention is important. In addition to adequate biliary drainage for jaundice reduction and cholangitis prevention, portal vein branch embolization has recently come to be performed aggressively [47]. The portal vein branch of the segment to be resected is embolized to promote the atrophy of that region and the compensatory hypertrophy of the predicted residual liver, and major hepatectomy is scheduled for a few weeks later [48-50]. The catheter is inserted by puncture for ultrasound-guided percutaneous transhepatic portal embolization (PTPE) [51,52] or by direct puncture of the ileocolic vein through a small laparotomy. A fibrin glue, ethanol, variceal sclerosing agent, Gelfoam, and embolizing coil are used as embolizing material. It is necessary to prevent the regurgitation of embolizing material, to embolize the site a little away from the predicted residual liver (as an inflammatory reaction may occur and make portal vein separation difficult), and to consider re-embolization if early re-canalization occurs in the embolized portal vein branch[53].

Diagnosis

To determine the surgical technique, it is important to determine the extent of cancer invasion. Nimura et al. analyzed the results of cholangiography, CT, and percutaneous transhepatic cholangioscopy (PTCS) in detail, diagnosed cancer invasion of caudate lobe bile-duct branches preoperatively, determined the liver segment to be resected, and performed combined hepatic segmentectomy and caudate lobectomy, thereby improving the curable resection rate and treatment results. Among various examinations, direct cholangiography by PTBD remains the current gold standard for the diagnosis of the degree of extension in the long (horizontal) axis of the bile duct [54], which is most important for surgical technique selection, and the fundamental diagnosis of the degree of extension is made by interpreting the narrowing, sclerosis, and irregularity of the bile duct wall. In this regard, sufficient care should be taken not to aggravate the general condition by segmental cholangitis due to excessive imaging [55]. Our department performs PTBD as the fundamental preoperative jaundice-reducing procedure, diagnosis the degree of extension of hilar cholangiocarcinoma mainly by direct cholangiography, clarifies the anatomical characteristics of the vessels in individual patients by 3D-CT, and performs PTPE according to the hepatic reserve, thereby trying to more safely perform extended resection to increase the radical curability of hilar cholangiocarcinoma.

Resected patients

The mode of local extension of hilar cholangiocarcinoma is generally described as that in the vertical and horizontal directions [56-59]. The degree of extension strongly influences the degree of cancer progression, that is, the prognosis. Regarding vertical extension, early biliary cancers, which are not exposed on the serosal surface, with an invasion depth of m or fm, and those with an invasion depth of ss have a better prognosis than those with a greater depth of invasion. However, as evident from the anatomical charac-

teristics of the hilar bile ducts, cancers that have extended outside the wall of bile ducts tend to directly invade the anatomically adjacent liver parenchyma and vascular wall. In this regard, the histopathological parameters pHinf, pPV, and pA come into question, strongly influence the possibility of curable resection, and become major factors leading to pEM-positivity in resected patients [56]. Cancer extension in the horizontal direction, that is, in the upper and lower directions along the long axis of bile ducts, is also frequently observed, and comes into question in determining the extent of surgical resection. The mode of extension in the horizontal direction is divided into extension in the stroma (ly, v, pn) and that in the bile duct wall. The superficial extension type [60], which extends by replacing epithelium without duct wall thickening, and is difficult to recognize by imaging modalities, as well as a skip lesion [61], is rarely observed. Tumor cells are sometimes observed to extend in the stroma beyond the invasive front of the main tumor. These patterns of horizontal extension contribute to making it difficult to determine the extent of resection based on a negative resection margin (pHM, pDM). Some studies have reported that PTCS [62] and intraductal ultrasound (IDUS) [61] are useful to diagnose the degree of extension of the superficial extension type and skip lesion, while other studies have noted that the placement of a PTBD catheter makes it difficult to determine the boundary of the lesion because of bile-duct wall thickening and mucosal denuding [63-65], requiring precautions.

In this study, the group negative for both parameters (pHM, pEM) related to the resection margin had a significantly better prognosis. The node metastasis-negative group tended to have a better prognosis, with no significant difference in the survival rate, suggesting that even if lymph node metastasis is observed before or during surgery, effective (residual tumor-free) lymph node dissection would lead to curability, promising a good prognosis. Since no effective adjuvant therapy for cholangiocarcinoma has been established to date, these results indicate the critical importance of performing surgery achieving final curability A or B. Unfortunately, multivariate analysis yielded no significant results regarding which histopathological parameters most strongly influenced the cumulative survival rate. We are considering further studies in more patients to aid in the determination of a treatment policy for hilar cholangiocarcinoma.

In conclusion, patients with an early, histologically well-differentiated hilar cholangiocarcinoma who have undergone surgery achieving final curability A or B can be expected to have a good long-term prognosis. Therefore, it is important not only to aim at early detection, but also to determine the extent of resection and surgical technique based on the accurate evaluation of cancer extension.

ACKNOWLEDGMENTS: We thank Prof. S. Aoyagi for his thoughtful review of this manuscript. We are also grateful to Prof. T. Kinoshita for his constant guidance and manuscript review, and to Prof. Emeritus T. Nakayama for his helpful advice. We are indebted to members of our laboratory for their cooperation in this work.

REFERENCES

1. Japanese Society of Biliary Surgery. General Rules for Surgical and Pathological Studies on Cancer of the Biliary Tract, 5th edn, Kanehara, Tokyo, pp 1-65, 2003. (in Japanese)
2. Mizumoto R. Treatment strategy for hilar carcinoma of the bile duct. Geka Chiryo 1999; 80:1255-1256. (in Japanese)
3. Klatskin G. Adenocarcinoma of hepatic duct at the bifurcation within the porta hepatis. An usual tumor; distinctive clinical and pathological features. Am J Med 1965; 38:241-256.
4. Nimura Y. Treatment of hilar cholangiocarcinoma; present and future perspective. Geka 2003; 65:663-668. (in Japanese)
5. Couinaud C. Surgical anatomy of the liver revisited. self-publication, Paris, pp 39-53, 1989.
6. Taoka D, and Kawarada Y. Surgical anatomy of the hepatic hilar area. J Jpn Surg Soc 2000; 101:386-392. (in Japanese)
7. Ishiyama S, Yamada S, Narushima Y, Yamaki T, Kunii Y et al. Surgical anatomy of the hilar bile duct. J Bil Panc 1999; 20:811-820. (in Japanese)
8. Nimura Y, Kamiya S, Kondo S, Nagino M, Uesaka K et al. Aggressive preoperative management and extended surgery for hilar cholangiocarcinoma; Nagoya experience. J Hepatobiliary Pancreat Surg 2000; 7:155-162.
9. Nakeeb A, Pitt HA, Sohn TA, Coleman J, Abrams RA et al. Cholangiocarcinoma. A spectrum of intrahepatic, perihilar, and distal tumors. Ann Surg 1996; 224:463-475.
10. Miyazaki M, Ito H, Nakagawa K, Ambiru S, Shimizu H et al. Aggressive surgical approaches to hilar cholangiocarcinoma; hepatic or local resection? Surgery 1998; 123:131-136.
11. Burke EC, Jarnagin WR, Hochwald SN, Pisters PW, Fong Y et al. Hilar cholangiocarcinoma; patterns of spread, the importance of hepatic resection for curative operaton, and a presurgical clinical staging system. Ann Surg 1998; 228:385-394.
12. Brown G. Surgical removal of tumors of the hepatic duct. Postgrad Med 1954; 16:79-85.
13. Longmire WP Jr, and Lippman HN. Intrahepatic cholangiojejunostomy-an operation for biliary obstruction. Surg Clin N Amer 1956; 36:849-863.
14. Terblanche J, Saunders SJ, and Louw JH. Prolonged palliation in carcinoma of the main hepatic duct junction. Surgery 1972; 71:720-731.

15. Cameron JL, Broe P, and Zuidema GD. Proximal bile duct tumors; surgical management with silastic transhepatic biliary stents. Ann Surg 1982; 196:412-419.
16. Hart MJ, and White TT. Central hepatic resection and anastomosis for stricture or carcinoma at the hepatic bifurcation. Ann Surg 1980; 192:299-304.
17. Mistilis S, and Schiff L. A case of jaundice due to unilateral hepatic duct obstruction with relief after hepatic lobectomy. Gut 1963; 4:13-15.
18. Quattlebaum JK, and Quattlebaum JK Jr. Malignant obstruction of the major hepatic ducts. Ann Surg 1965; 161:876-899.
19. Bird AD, Kerr GD, and Wynne-Jones G. Hepatic lobectomy for carcinoma of the hepatic duct. NZ Med J 1971; 73:351-354.
20. Haynes CD, Gingrich GW, and Thorougham JC. Carcinoma of the bile duct; diagnosis and treatment. Am Surg 1964; 30:578-582.
21. Cady B, and Fortner JG. Surgical resection of intrehepatic bile duct cancer. Am J Surg 1969; 118:104-107.
22. Longmire WP, McArthur MS, Bastounis EA, and Hiatt J. Carcinoma of the extrahepatic biliary tract. Ann Surg 1973; 178:333-343.
23. Fortner JG, Kinne DW, Kim DK, Castro EB, Shiu MH et al. Vascular problems in upper abdominal cancer surgery. Arch Surg 1978; 109:148-153.
24. Tsuzuki T, Ogata Y, Iida S, Nakanishi I, Takenaka Y et al. Carcinoma of the bifurcation of the hepatic ducts. Arch Surg 1983; 118:1147-1151.
25. Sakaguchi S, and Nakamura S. Surgery of the portal vein in resection of cancer of the hepatic hilus. Surgery 1986; 90:344-349.
26. Nimura Y, Hayakawa N, Kamiya J, Maeda S, Kondo S et al. Combined portal vein and liver resection for carcinoma of the biliary tract. Br J Surg 1991; 78:727-731.
27. Blumgart LH, Drury JK, and Wood CB. Hepatic resection for trauma, tumor and biliary obstruction. Br J Surg 1979; 66:762-769.
28. Mizumoto R, Kawarada Y, and Suzuki H. Surgical treatment of hilar carcinoma of the bile duct. Surg Gynecol Obstet 1986; 162:153-158.
29. Iwasaki Y, Okamura T, Ozaki A, Todoroki T, Takase Y et al. Surgical treatment for carcinoma at the confluence of the major hepatic ducts. Surg Gynecol Obstet 1986; 162:457-464.
30. Nimura Y, Hayakawa N, Kamiya J, Kondo S, and Shionoya S. Hepatic segmentectomy with caudate lobe resection for bile duct carcinoma of the hepatic hilus. World J Surg 1990; 14:535-544.
31. Suzuki H. Correlation and abnormalities of the blood vessels in Glisson's capsule: From the standpoint of hepatobiliary surgery. Nihon geka hokan 1982; 51:713-731. (in Japanese)
32. Kumon M. Problems in surgical treatment of hilar cholangiocarcinoma in relation to cancer extension into the caudate lobe biliary tree. Kanzo 1985; 26:1193-1199. (in Japanese)
33. Nimura Y, Hayakawa N, Hasegawa Y, Kamiya J, Kondo S et al. Problems in surgical treatment of hilar cholangiocarcinoma as judged from the degree of extension to caudate lobe bile-duct branches. J Jpn Surg Soc 1986; 87:1094-1097. (in Japanese)
34. Mizumoto R, and Suzuki H. Surgical anatomy of the hepatic hilum with special reference to the caudate lobe. World J Surg 1988; 12:2-10.
35. Kamiya J, Nimura Y, Hayakawa N, Maeda S, and Kondo S. Preoperative cholangiography of the caudate lobe; surgical anatomy and staging for biliary carcinoma. J Hepatobiliary Pancreat Surg 1994; 1:385-389.
36. Couinaud C. The paracaval segments of the liver. J Hepatobiliary Pancreat Surg 1994; 1:145-151.
37. Nimura Y. Surgical regional anatomy of the caudate lobe: Segments I and IX. J Bil Panc 1996; 17:1189-1196. (in Japanese)
38. Nimura Y, Hayakawa N, Kamiya J, Maeda S, Kondo S et al. Hilar cholangiocarcinoma; surgical anatomy and curative resection. J Hepatobiliary Pancreat Surg 1995; 2:239-248.
39. Su CH, Tsay SH, Wu CC, Shyr YM, King KL et al. Factors influencing postoperative morbidity, mortality, and survival after resection for hilar cholangiocarcinoma. Ann Surg 1996; 223:384-394.
40. Mizumoto R, Ogura Y, and Akasaka Y. Feature article: Surgery of bile duct cancer: Current status and problems of resection results. J Jpn Surg Assoc 1984; 39:1383-1388. (in Japanese)
41. Imayama H, Kinoshita H, Okuda K, Hara M, Hasuta K et al. Surgical treatment for hilar bile duct carcinoma. Geka Chiryo 1997; 76:845-848. (in Japanese)
42. Nakayama T, Ikeda A, and Okuda K. Percutaneous transhepatic drainage of the biliary tract. Technique and results in 104 cases. Gastroenterology 1977; 74:708-714.
43. Nagino M, Nimura Y, and Kamiya J. Preoperative management of hilar cholangiocarcinoma. J Hepatobiliary Pancreat Surg 1995; 2:215-223.
44. Sato T, Andoh H, Shibata S, Yasui O, Yoshioka M et al. Current standard treatments for hilar bile duct carcinoma. Geka 2001; 63:1565-1571. (in Japanese)
45. Nimura Y, Kamiya J, Kondo S, Nagino M, and Kanai M. Technique of inserting multiple biliary drains and management. Hepatogastroenterology 1995; 42:323-331.
46. Nagino M, Kamiya J, Uesaka K, Sano T, Yamamoto H et al. Complications of hepatectomy for hilar cholangiocarcinoma. World J Surg 2001; 25:1277-1283.
47. Makuuchi M, Thai BL, Takayasu K, Takayama T, Kosuge T et al. Preoperative portal embolization to increase safety of major hepatectomy for hilar bile duct carcinoma: a preliminary report. Surgery 1990; 107:521-527.
48. Nagino M, Nimura Y, Kamiya J, Kondo S, Uesaka K et al. Changes in hepatic lobe volume in biliary tract cancer patients after right portal vein embolization. Hepatology 1995; 21:434-439.
49. Uesaka K, Nimura Y, and Nagino M. Changes in hepatic lobar function after right portal vein embolization; an appraisal by biliary indocyanine green excretion. Ann Surg 1996; 223:77-83.
50. Nagino M, Kamiya J, Kanai M, Uesaka K, Sano T et al. Right trisegment portal vein embolization for biliary tract carcinoma: technique and clinical utility. Surgery 2000; 127:155-160.

51. Nagino M, Nimura Y, and Hayakawa N. Percutaneous transhepatic portal embolization using newly devised catheters: preliminary report. World J Surg 1993; 17:520-524.
52. Nagino M, Nimura Y, Kamiya J, Kondo S, and Kanai M. Selective percutaneous transhepatic embolization of the portal vein in preparation for extensive liver resection: the ipsilateral approach. Radiology 1993; 200:559-563.
53. Goto Y, Nagino M, and Nimura Y. Doppler estimation of portal blood flow after percutaneous transhepatic portal vein embolization. Ann Surg 1998; 228:209-213.
54. Shimizu H, Ito H, Kimura F, Togawa A, Ohtsuka M et al. Cholangiographic Diagnosis of Cancer Extension for Hilar Cholangiocarcinoma. Syoukakigazo 2004; 6:373–379. (in Japanese)
55. Kamiya J, and Nimura Y. Selective cholangiography ② Hilar cholangiocarcinoma. Syoukakigazo 1999; 1:435-439. (in Japanese)
56. Nagai H, Kuroda K, Wada Y,Morioka Y, Noro T et al. Pathology of Bile Duct Carcinoma at the Hepatic Hilus–Modes of Spread. J Bil Panc 1984; 5:1469-1481. (in Japanese)
57. Nagakawa T, Kitagawa H, Kayahara M, Ohta T, and Konishi I. Spreading patterns of hilar bile duct cancer. J Jpn Surg Soc 2000; 101:399-403. (in Japanese)
58. Ebata T, Watanabe H, Ajioka Y, Nishikura K, Date K et al. Extrahepatic Bile Duct Cancer: Correlation between macroscopic appearance and mode of spread. Syoukakigazo 1999; 1:165–172. (in Japanese)
59. Nagakawa T, and Ohta T. The mode of spread of extrahepatic bile Duct carcinoma. J. Bil. Panc. 1990; 11:333-338. (in Japanese)
60. Ojima H, and Sakamoto M. Clinicopathological features of hilar cholangiocarcinoma. Syoukakigazo 2004; 6:345-351. (in Japanese)
61. Kai M, Chijiiwa K, Tsuchiya K, Ouchida J, Eto T et al. A case of hilar bile duct cancer with skip lesion diagnosed correctly by intraductal ultrasonography (IDUS). J J B A 2004; 18:531-539. (in Japanese)
62. Maguchi H, Takahashi K, Katanuma A, T hayashi, A Yoshida et al. Evalustion of tumor extent and selection of surgical treatment for bile duct carcinomas. Syoukakigazo 2003; 5:367-374. (in Japanese)
63. Tamada K, Tomiyama T, Ichiyama M, Ohashi A, Wada S et al. Influence of biliary drainage catheter on bile duct wall thickness as measured by intraductal ultrasonography. Gastrointest Endosc 1998; 47:28-32.
64. Tamada K, Kanai N, Wada S, Tomiyama T, Ohashi A et al. Utility and limitations of intraductal ultrasonography in distinguishing longitudinal cancer extension along the bile duct from inflammatory wall thickening. Abdom Imaging 2001; 26:623-631.
65. Kamiya J, Nishio H, Arai T, Oda T, Nagino M et al. Indication of percutaneous transhepatic cholangioscopy (PTCS) and cholangioscopic biopsy. J Bil Panc 2003; 24:433-437. (in Japanese)